Cyclic-AMP Dynamics and Heterogeneity in *Mycobacterium tuberculosis*: Insights into Host-Pathogen Interactions

A Thesis

submitted to

Indian Institute of Science Education and Research Pune in partial fulfilment of the requirements for the BS-MS Dual Degree Programme

by

Srivathsa S Kurpad

Indian Institute of Science Education and Research Pune

Dr. Homi Bhabha Road,

Pashan, Pune 411008, INDIA.

Date: April 2025

Supervisor: Dr Neeraj Dhar,

Principal Scientist, Vaccine and Infectious Disease Organization, University of Saskatchewan, Canada

From June 2024 to March 2025

INDIAN INSTITUTE OF SCIENCE EDUCATION AND RESEARCH PUNE

Certificate

This is to certify that this dissertation entitled “Cyclic-AMP Dynamics and Heterogeneity in *Mycobacterium tuberculosis*: Insights into Host-Pathogen Interactions” towards the partial fulfilment of the BS-MS dual degree programme at the Indian Institute of Science Education and Research, Pune represents work carried out by Srivathsa S Kurpad at the Centre for Infectious Disease Research, Indian Institute of Science, Bangalore under the supervision of Dr Amit Singh, Professor, Centre for Infectious Disease Research (CIDR) and Department of Microbiology and Cell Biology (MCBL), Indian Institute of Science and Dr Neeraj Dhar, Principal Scientist, Vaccine and Infectious Disease Organization, University of Saskatchewan, Canada, during the academic year 2024-2025.

Dr Neeraj Dhar

Committee:

Dr Neeraj Dhar 

Dr Amit Singh 

Dr Sunish Kumar Radhakrishnan 

This thesis is dedicated to Neeraj

Declaration

I hereby declare that the matter embodied in the report entitled “Cyclic-AMP Dynamics and Heterogeneity in *Mycobacterium tuberculosis*: Insights into Host-Pathogen Interactions” are the results of the work carried out by me at the Centre for Infectious Disease Research, Indian Institute of Science, Bangalore, under the supervision of Dr Neeraj Dhar and the same has not been submitted elsewhere for any other degree

Srivathsa S Kurpad

Date: 12th March 2025

Table of Contents

List of Tables

List of Figures

Abstract

3′,5′-Cyclic adenosine monophosphate (cAMP) is a nucleotide secondary messenger molecule widely used across biological domains. While it has been implicated in several crucial physiological processes of *Mycobacterium tuberculosis,* including virulence, resuscitation from dormancy, adaptation to stresses, and antibiotic tolerance, its temporal dynamics and heterogeneity remain unexplored. Using a novel fluorescent biosensor for cAMP, rmgCarvi, we assessed the temporal dynamics of intramycobacterial cAMP during resuscitation from dormancy and dormancy-like states, in response to physiologically relevant stresses *in vitro*, and during infection in RAW264.7 macrophages. We demonstrate a rapid and large increase in intramycobacterial cAMP levels during resuscitation from nutrient starvation-induced dormancy, independent of the presence of exogenous free fatty acids and reveal new insights into the kinetics of this phenomenon. We also investigated cAMP levels upon infection in RAW264.7 macrophages and confirmed the previously reported increase in intramycobacterial cAMP levels. To delineate the host microenvironment behind this burst, we explored intramycobacterial cAMP dynamics in response to combined acid and salt stress *in vitro*, generating new insights on the nature of their synergistic regulation. Additionally our studies reveal that acidic pH of the phagosome is not the major driver of increased intramycobacterial cAMP production and revealed tight temporal regulation over the cAMP burst. In conclusion our studies using the cAMP fluorescent reporter strain reveal fundamental insights into general principles of cAMP signalling and regulation in response to stresses and during infection.

Acknowledgments

The past year has been one wherein every week brought a uniquely different challenge. I am filled with a sense of confidence and pride, knowing that I was able to navigate trying times while simultaneously discovering a genuine passion for science. This journey of growth was facilitated by a star-studded cast of numerous individuals to whom I am forever indebted.

To Neeraj, words cannot do justice to my gratitude for you. You have been a constant source of support, both personally and professionally, and stimulation over the past two years and guided me through the process of finding my academic passion expertly. Your patience and understanding are second to none, and I would be hard-pressed to ever find a more perfect mentor.

I am immensely grateful to Amit Sir for welcoming me into his lab and giving me the opportunity and freedom to grow scientifically through the project. The lab environment, particularly during the meetings, dramatically deepened my passion for science. Navigating the process of conceptualising and executing experiments individually has been an incredibly valuable learning experience. To Madhura and Rohit, your incredible mentorship gave me the confidence to ideate and execute experiments self-sufficiently. To Hussain, thank you for always lending a helping hand and answering every last of my questions. To everyone at ASL, I thank you for creating an inviting and stimulating environment, one that I looked forward to returning to every day. I would also like to thank Nagasuma Ma'am for being a constant source of personal support and for going out of her way to fight for me.

It would have been impossible for me to make it through the last year without the family we chose – Devdas, Omkar, Niranjan, Kritin, Ved, Ram, Shravan, Anmol, Aashray, and Ashutosh – who were an infinite source of fun and love. FIFA and snooker (shoutout to Giri Anna and Hikmath Bhai) have been *af*. I am an awe of the amount we have all grown as individuals and closer collectively. My friends at IISER – Anuj, Surya, Nikhil, Manav, Yatish, Giri, Maro, Pooja, and Krishna – were everything and more that I could have ever asked for. I cherish the uniquely special relationship I formed with each of you. It has been an absolute blessing.

My parents and sister have been undying pillars of support and help. To them, I owe everything. And to Prekshitha, thank you for always being in my corner; you are my world.

Contributions

Contributor name	Contributor role
Dr Neeraj Dhar, Dr Amit Singh, Srivathsa S Kurpad	Conceptualization
Dr Neeraj Dhar, Dr Amit Singh, Srivathsa S Kurpad	Methodology
-	Software
Srivathsa S Kurpad	Validation
Srivathsa S Kurpad	Formal analysis
Srivathsa S Kurpad	Investigation
Dr Neeraj Dhar, Dr Amit Singh	Resources
Srivathsa S Kurpad	Data Curation
Srivathsa S Kurpad	Writing - original draft preparation
Srivathsa S Kurpad, Dr Neeraj Dhar	Writing - review and editing
Srivathsa S Kurpad	Visualization
Dr Neeraj Dhar, Dr Amit Singh	Supervision
Dr Neeraj Dhar, Dr Amit Singh, Srivathsa S Kurpad	Project administration
Dr Neeraj Dhar, Dr Amit Singh	Funding acquisition

This contributor syntax is based on the Journal of Cell Science CRediT Taxonomy[1].

[1] https://journals.biologists.com/jcs/pages/author-contributions

Chapter 1 **Introduction**

Secondary Messengers and Host-Pathogen Crosstalk

Signal transduction is an essential process by which organisms sense their environments and mount an appropriate response (Thorner *et al.*, 2014; Newton *et al.*, 2016). Molecules that are present in the environment, termed primary messengers, bind to receptors on the cell's surface, kicking off a series of biochemical reactions called a signalling cascade. A group of small intracellular molecules, termed secondary messengers, transduce the signalling cascade from the cell-surface receptors to effector proteins, bringing about a response to the environmental stimuli through a cellular response. Numerous molecules have been identified to function as secondary messenger molecules in a variety of cell types, including cyclic mono- and di-nucleotides, alarmones, inositol triphosphate, diacylglycerol, and Ca2+ (Newton *et al.*, 2016).

Bacteria have evolved to develop numerous mechanisms to respond to environmental cues in a rapid manner. This is a necessity due to the diverse, variable, and often hostile environments they reside in. These mechanisms include chemotaxis (Armitage, 1992; Porter *et al.*, 2011); mechanosensing (Persat *et al.*, 2015; Gordon and Wang, 2019); and signal transduction through receptors and secondary messengers along with two-component systems (TCS) (Laub and Goulian, 2007; Hengge, 2009; Alvarez and Georgellis, 2023). The ability of a bacterium to sense and adapt to its surroundings is especially crucial for the survival of bacterial pathogens in an immunocompetent host (Thakur *et al.*, 2019). Over the course of evolution, pathogens and the host's immune system have co-evolved to orchestrate a complex interaction between the two that is characterized by the exchange of molecular signals that facilitate both pathogenesis and an appropriate immune response. Given the hostile nature of their niche, intracellular pathogens have developed sophisticated mechanisms to modulate their physiology and enable their survival and virulence by sensing host-derived signals (Huynh and Grinstein, 2007; Dey and Bishai, 2014; Reniere *et al.*, 2016; Anderson *et al.*, 2018; Thakur *et al.*, 2019). Secondary messenger molecules have been shown to play a critical and dynamic bidirectional role in host-pathogen crosstalk pathogen (Dey and Bishai, 2014; Thakur *et al.*, 2019).

A stereotypical example of this complex host-pathogen dynamic is tuberculosis (TB), caused by the infection of a susceptible host by *Mycobacterium tuberculosis* (Mtb). Once the bacilli are inhaled, they reside intracellularly within alveolar macrophages, neutrophils, and dendritic cells following phagocytosis (Eum *et al.*, 2010; Philips and Ernst, 2012). A complex and multifactorial chemical dialogue between the bacilli and host cell ensues, with numerous host and bacterial factors influencing the infection outcome (Dey and Bishai, 2014; Toniolo *et al.*, 2021). To survive and thrive in this intracellular niche, Mtb utilizes host nutrients and, senses and responds to its environment by leveraging a combination of two-component systems and secondary messenger signalling pathways (Chao *et al.*, 2010; Dey and Bishai, 2014; Knapp and McDonough, 2014; Parish, 2014; Prisic and Husson, 2014; Johnson and McDonough, 2018; Huang *et al.*, 2019; Russell *et al.*, 2019; Stupar *et al.*, 2022). A successful infection is characterized by Mtb's survival in macrophage phagosomes by blocking phagosome maturation and acidification, and phago-lysosomal fusion. Once the adaptive immune response is activated, a well-organised host immune structure called the granuloma forms to contain the bacilli. The granulomatous response could lead to sterilizing immunity by the clearance of the bacteria, to containment of the bacteria, resulting in a state of prolonged dormancy, or to caseation and necrosis, which releases virulent bacteria out of the granuloma allowing for relapse of the infection and facilitating transmission to other hosts (Philips and Ernst, 2012).

cAMP Signalling in *Mycobacterium tuberculosis*

3′,5′-cyclic-AMP (cAMP) is a nucleotide secondary messenger molecule. It is synthesized by adenylyl cyclases (ACs) from adenosine triphosphate (ATP) and degraded by phosphodiesterases (PDEs) to adenosine monophosphate (AMP). Its function was initially identified in the context of hormonal signal transduction pathways. However, it has since been shown to be implicated in regulating aspects of metabolism signalling, memory formation, and innate immune responses in the mammalian system (Kresge *et al.*, 2005; Serezani *et al.*, 2008; Altarejos and Montminy, 2011). In the context of bacteria, virulence, gene expression during infection, and catabolite repression in *E. coli*, a regulatory mechanism allowing bacteria to utilize a preferred carbon source selectively, have all been shown to be regulated by cAMP (Görke and Stülke, 2008; McDonough and Rodriguez, 2011).

Mycobacterium tuberculosis is unique in the prokaryotic world for its dependence on cAMP signalling, with around 1% of its genome predicted to interact with cAMP (Wong *et al.*, 2023). Mtb encodes over 16 class III ACs, while most other prokaryotic organisms encode just one. A catalytic core characterizes the adenylyl cyclases, but some also include regulatory domains. The catalytic core enables the biosynthesis of cAMP. The regulatory domains regulate cAMP production in response to certain physiologically relevant environmental stimuli, including pH, nutrient sources such as fatty acids, carbon dioxide, and hypoxia (Dey and Bishai, 2014; Knapp and McDonough, 2014; Johnson and McDonough, 2018). This indicates that cAMP plays a crucial role in regulating Mtb's physiology in response to the dynamic environments it is exposed to during its lifetime in a host. Two genes have been identified that encode phosphodiesterases that break down cAMP - *rv0805* (Shenoy *et al.*, 2007) and *rv1339* (Thomson *et al.*, 2022). The catalytical activity of *Rv0805* has been shown to be higher for 2′,3′-cAMP (an RNA degradation product) in comparison to 3′,5′-cAMP (Keppetipola and Shuman, 2008; McDowell *et al.*, 2023), whereas this difference is not seen in the case of *R*v1339 (Thomson *et al.*, 2022).

In Mtb, cAMP binds to effector proteins, termed cyclic nucleotide monophosphate (cNMP) binding proteins. Eleven have been identified; however, only a few have been well-studied (Knapp and McDonough, 2014; Johnson and McDonough, 2018; McDowell *et al.*, 2023). *rv0998*/KATmt/Mt-Pat is a cAMP-dependent protein lysine acetyltransferase (Nambi *et al.*, 2013). The transcription factors *rv3676* (cAMP responsive protein of Mtb (CRPmt)) and *rv1675c* (cAMP and macrophage regulator (cmr)) regulate gene expression in Mtb in a cAMP-dependent manner (Rickman *et al.*, 2005; Gazdik *et al.*, 2009). *Rv1636* has been identified as an essential universal stress protein that is able to modulate cAMP levels in Mtb by binding to and sequestering cAMP (Banerjee *et al.*, 2015, 2024).

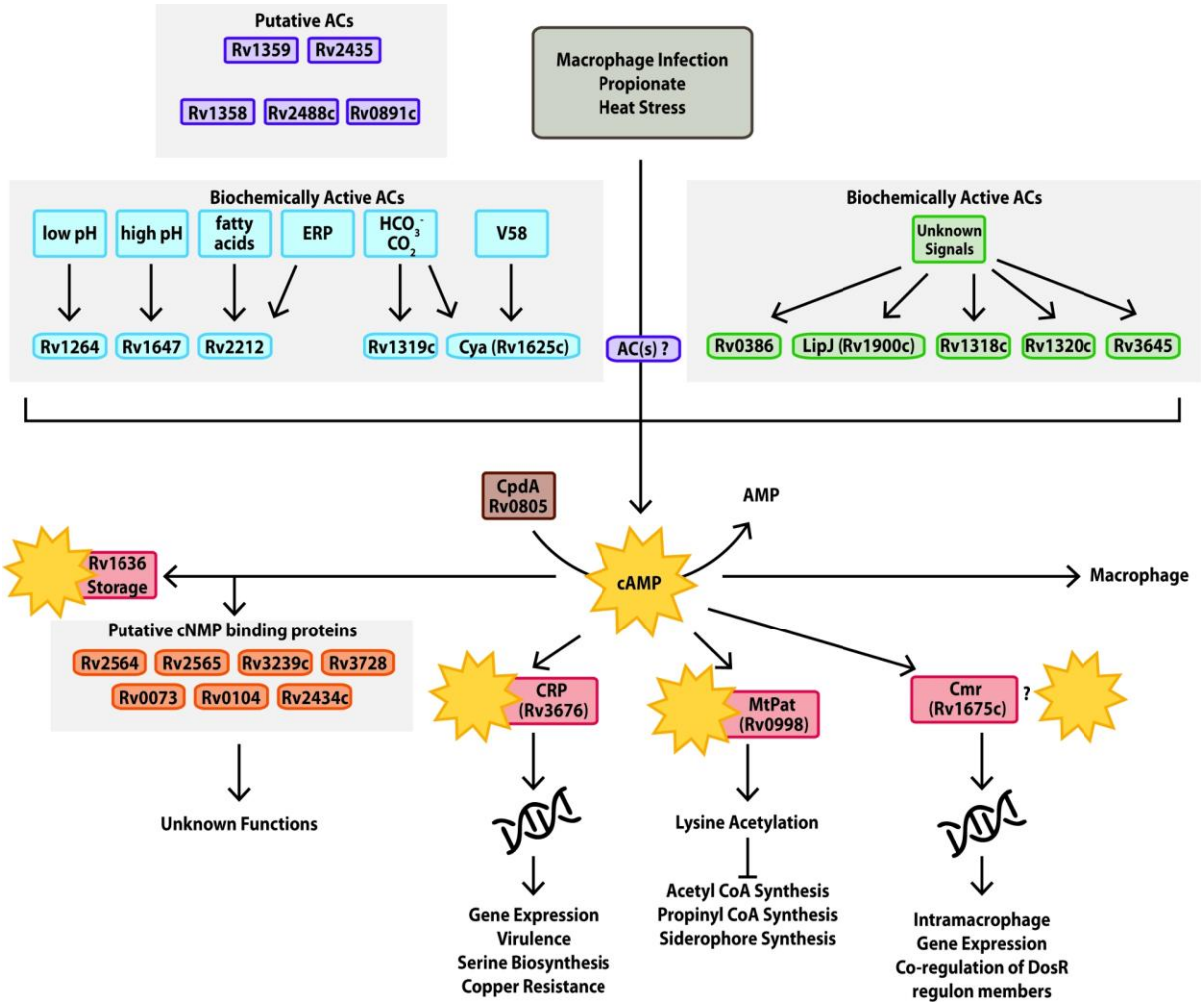

Figure 1: *Cyclic-AMP signalling in Mycobacterium tuberculosis.* The figure is reproduced from (Johnson and McDonough, 2018)**.**

Roles of cAMP during *Mycobacterium tuberculosis* Infection in Macrophages

A dynamic and dramatic change in the cAMP landscape occurs upon the internalization of Mtb by the host macrophage. cAMP modulates the physiology of the macrophage by binding to the Protein Kinase A (PKA) complex, which liberates kinase subunits, resulting in the phosphorylation and, therefore, activation of transcription factors (Knapp and McDonough, 2014). Upon Mtb's entry into J774.16 murine macrophages, a 50-fold increase in intramycobacterial cAMP levels has been reported. It is important to note the supraphysiological infective dose of an MOI (multiplicity of infection) of 200 that yielded this dramatic result (Bai *et al.*, 2009). Mtb has also been reported to expel cAMP into the host macrophage as a cAMP burst within 6 hours of infection. A cell wall-anchored adenylyl cyclase, *Rv0386*, mediates this phenomenon. Macrophage infection by Mtb has also been shown to activate

CREB (cAMP response element-binding protein). This activation is driven primarily by PKA (mediated by cAMP) and not by the other modalities of CREB activation – by p38 (mediated by lipopolysaccharide) or the ERK1/2 pathways (Agarwal *et al.*, 2009). cAMP has been shown to inhibit actin polymerization at the phagosomal membrane in a PKA-dependent manner (Kalamidas *et al.*, 2006). It has also been shown to down-regulate the necroptotic signalling pathway by preventing the phosphorylation of receptor-interacting protein kinase (RIPK) 3 and mixed lineage kinase domain like pseudokinase (MLKL) in a CREB-dependent manner (Leopold Wager *et al.*, 2023). Together, these pathways prevent of phagosome maturation and phago-lysosomal fusion, facilitating the survival of Mtb within early endosomes in the macrophage (Khan *et al.*, 2024). These results point towards a model (**Figure 2**) wherein phagocytosis of Mtb by macrophages initially induces a large increase in intramycobacterial cAMP levels, followed by a cAMP burst in the macrophage which serves to promote Mtb survival by actively preventing phagosome maturation, acidification, and fusion with the lysosome. This represents an additional mechanism by which Mtb successfully de-acidifies the phagosome it resides in, creating a permissive niche for itself within the host macrophage (Rohde *et al.*, 2007).

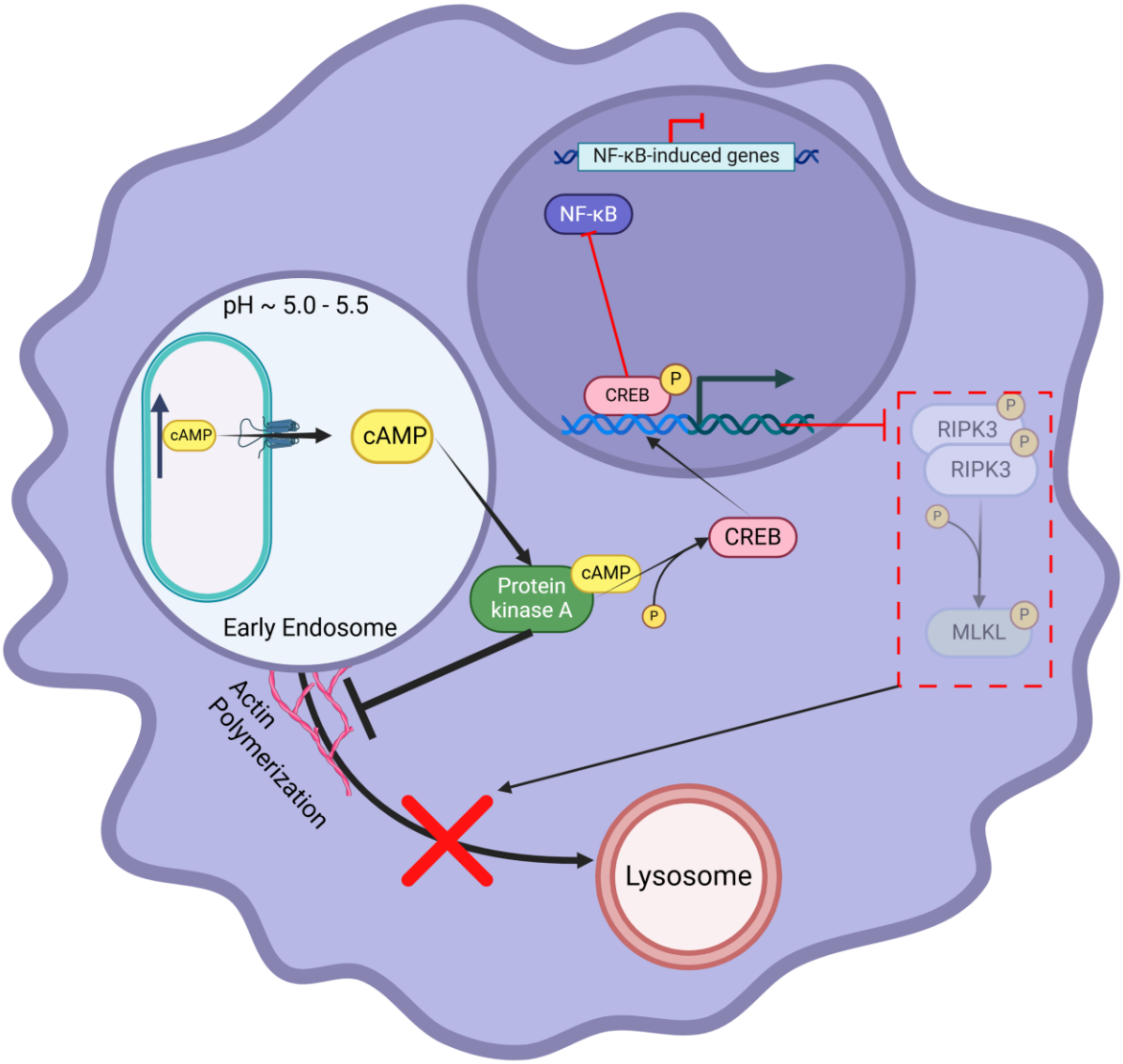

Figure 2: *cAMP-induced inhibition of phago-lysosomal fusion during Mycobacterium tuberculosis infection.* Abbreviations: cAMP – cyclic-AMP, CREB – cyclic-AMP response element binding protein, P – phosphate, NF-kB – Nuclear factor-kappa B, RIPK – receptor-interacting protein kinase, MLKL – mixed lineage kinase domain like pseudokinase. Created in https://BioRender.com.

Ratiometric gCarvi – the cAMP Biosensor

Despite the crucial nature of cAMP signalling in Mtb, relatively little is known about its heterogeneity and temporal dynamics during infection. The main reason for this lacuna in the field's understanding is the lack of a reliable and reproducible method to monitor cyclic-AMP levels in real time. The most prevalent methodologies employed to quantify cAMP levels in Mtb, or host cells include ELISA, luminosity,

radioimmunoassay-based detection mechanisms, or mass spectrometry. These assays, while accurate, require long sample preparation times, are incompatible with microscopy or cell sorting applications, and do not confer the ability to assay cAMP levels in real time or at the single cell level.

On the other hand, multiple fluorescence-based detection mechanisms for cAMP have been designed for use in eukaryotic systems. These include the use of FRET-based detection systems (Zaccolo *et al.*, 2000), cAMP biosensors (Harada *et al.*, 2017), ion channel-based reporter proteins, and fluorescent translocation reporters (ed. M Zaccolo, 2022), some of which are also compatible with *in vivo* studies (Kim *et al.*, 2008; ed. M Zaccolo, 2022). However, these cAMP fluorescent reporters have not yet been adapted for use in prokaryotic systems. To address these challenges, a cAMP-specific reporter protein originally designed for use in neuronal cells, gCarvi (Kawata *et al.*, 2022), was adopted and optimized for the prokaryotic system of *Mycobacteria* by our lab in 2023. gCarvi was developed by swapping the DNA-binding domain of the prokaryotic cAMP receptor protein (also called the catabolite activator protein (CAP) in *E. coli*) with the cyclically-permuted-GFP fluorophore (cpGFP) (**Figure 3A**). The reporter protein fluoresces (excitation peak at 504nm and emission peak at 523nm (**Figure 3B**)) upon binding to cAMP with rapid kinetics (**Figure 3D**). It has a significantly higher specificity for cAMP than cGMP (**Figure 3C** and **3E**). A ratiometric variant of gCarvi, called rmgCarvi, was engineered by fusing the mCherry fluorophore to gCarvi (**Figure 3F**). The mCherry fluorophore (excitation peak: 587nm, emission peak: 612nm) is constitutively fluorescent, and the cpGFP fluorophore (excitation peak: 500nm, emission peak: 525nm) fluoresces upon binding to cAMP (**Figure 3G**).

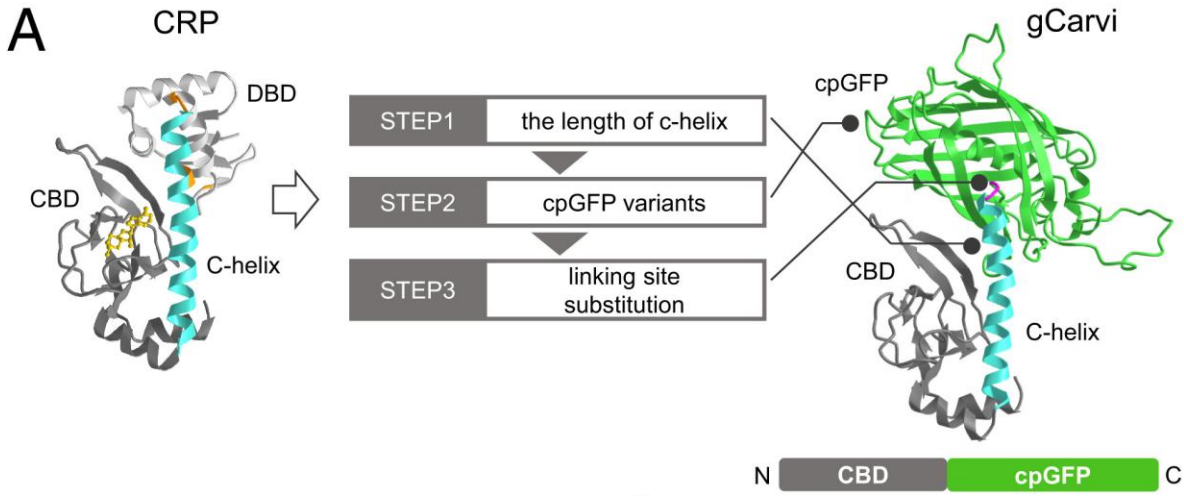

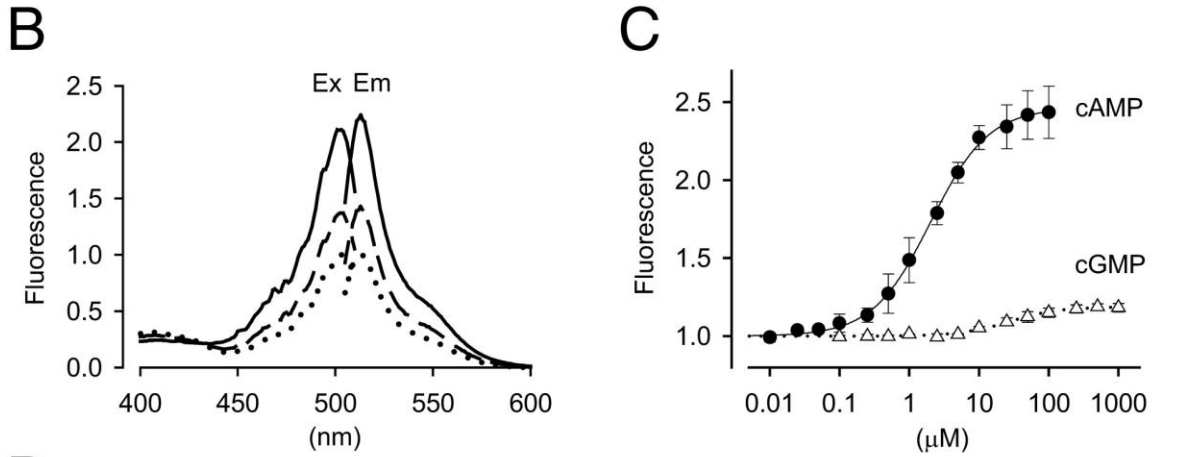

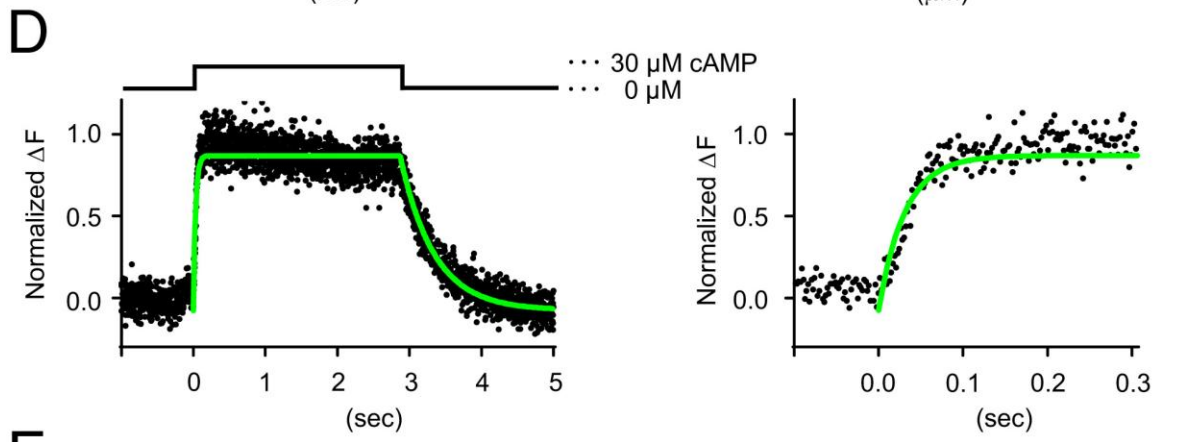

E

	cAMP					cGMP		
	K_d (μM)	n	D.R.	k_{on} ($M^{-1}s^{-1}$)	k_{off} (s^{-1})	K_d (μM)	n	D.R.
gCarvi	2.03	1.05	1.46	1.38×10^6	3.31	27.4	1.22	0.19

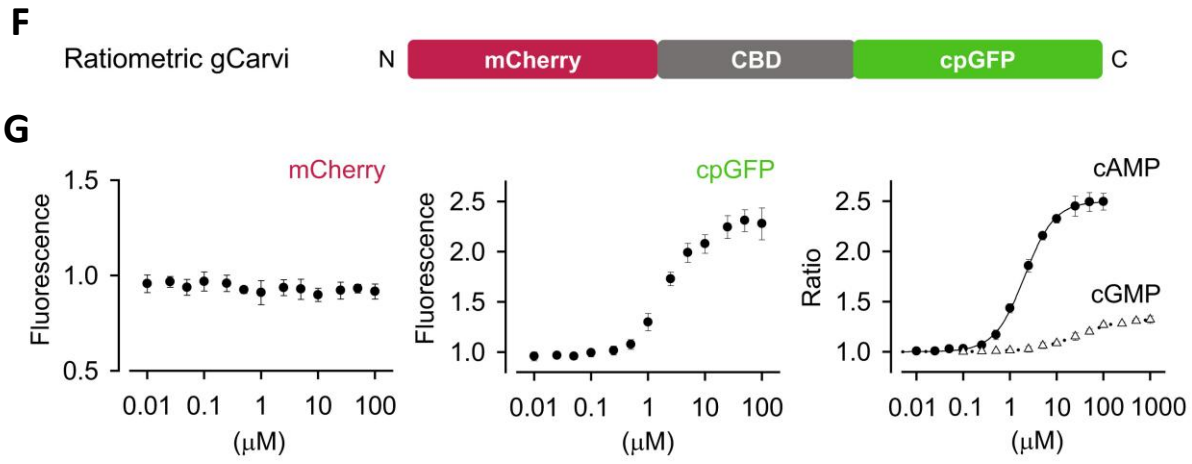

	cAMP					cGMP		
	K_d (μM)	n	D.R.	k_{on} ($M^{-1}s^{-1}$)	k_{off} (s^{-1})	K_d (μM)	n	D.R.
Ratiometric gCarvi	2.05	1.36	1.50	1.20×10^6	3.11	28.9	0.95	0.33

Figure 3: *Properties of gCarvi and ratiometric gCarvi (rmgCarvi) – fluorescent cAMP biosensors.* The figure is reproduced from *(Kawata* et al., *2022)*

Scope of the Thesis

We aim to investigate the temporal dynamics and kinetics of the cAMP signalling in *Mycobacterium tuberculosis* during resuscitation from dormancy, in response to physiologically relevant stresses such as acid and salt stress, and during infection in macrophages. This will be achieved by using the fluorescent cAMP biosensor rmgCarvi in combination with flow cytometry. This novel experimental approach aims to uncover fundamental insights into the temporal properties of cAMP signalling in *Mycobacterium tuberculosis*. These experiments will also validate the utility of rmgCarvi for assessing cytosolic cAMP levels in *M. tuberculosis.*

Chapter 2 **Materials and Methods**

Bacterial Strains and Growth Conditions

Mycobacterium smegmatis mc^2155 (Msm) and *Mycobacterium tuberculosis* H37Rv (Mtb) lab strains were grown in 7H9 broth (BD DIFCO 271310) supplemented with 0.2% glycerol, 0.05% Tween-80 (for Msm) or 0.05% Tyloxapol (for Mtb), and ADC (0.5% albumin – VWR amresco Life sciences 0332, 0.2% dextrose, 0.085% NaCl, 0.0004% Catalase – Sigma-Aldrich C9322) (hereafter referred to as bacterial culture media) with shaking at 180 rpm in a rotary shaker incubator or on 7H10/7H11 agar supplemented with OADC at 37 ^{o}C. OADC growth supplement used for experiments contained the above-described composition of ADC supplemented with 0.05% oleic acid (Sigma-Aldrich O1383).

Bacterial strains expressing ratiometric gCarvi (rmgCarvi) were generated by transforming the bacteria with the episomal, multicopy *E. coli*-mycobacterium shuttle vector pMV261 containing the rmgCarvi cyclic-AMP fluorescence sensor construct under the control of the rpsA promoter and a kanamycin resistance cassette (Tn903-derived aph gene) (**Figure 4**). Bacterial strains expressing rmgCarvi were grown in media containing kanamycin (SRL 25389-94-0) at a final concentration of 20 µg/mL.

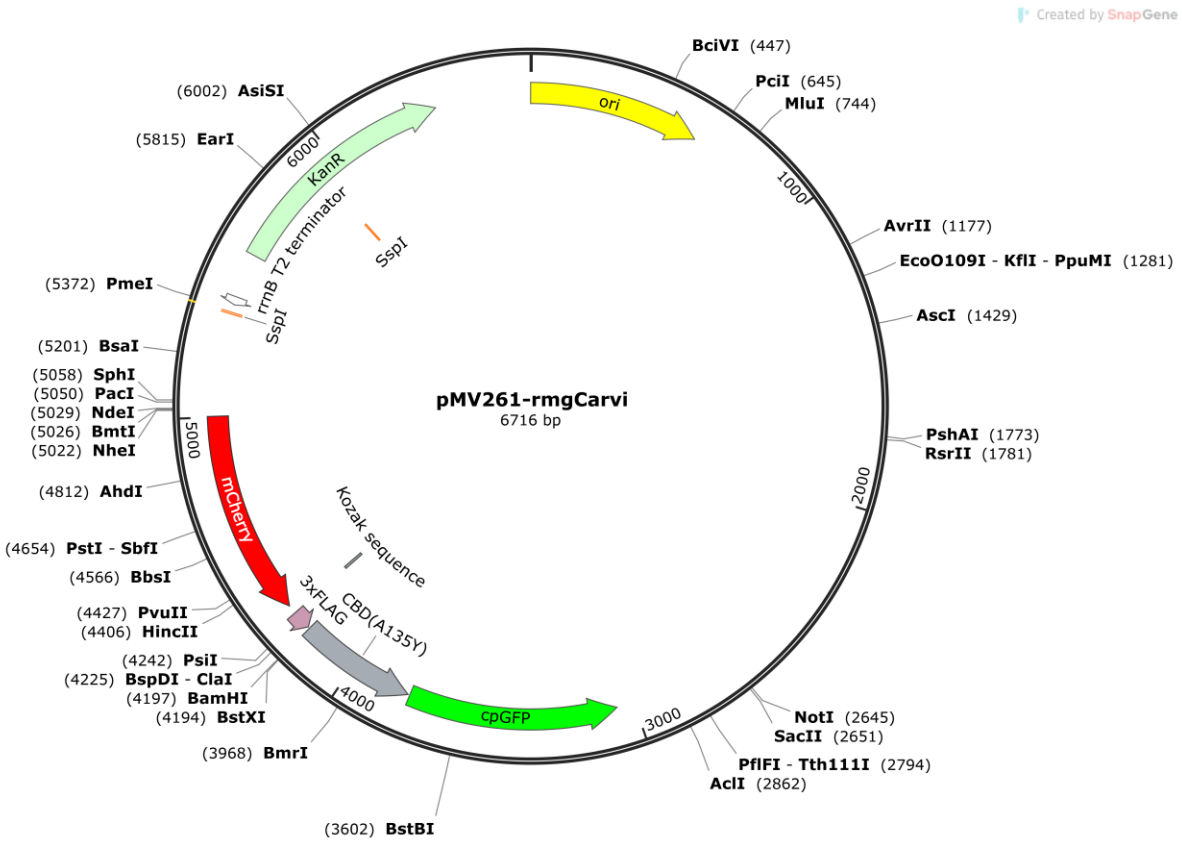

Figure 4: *Plasmid map of pMV261 containing the rmgCarvi construct.*

In order to modify the bacterial culture media from its regular pH of 6.6 to 5.5, 2-Morpholinoethanesulfonic acid (MES) was used at a concentration of 50mM to buffer the 7H9 so that it maintained an acidic pH of 5.5 upon the addition of HCl. The pH was confirmed using a pH meter [Mettler Toledo FiveEasy Plus]. Once the 7H9 reached the required pH, the required amount of ADC and Tyloxapol was added to complete the media. The media was then sterilized by passing it through a 0.2µm syringe filter aseptically in a biosafety cabinet.

Electroporation of DNA into Mycobacterium tuberculosis

Mtb was subcultured from a primary culture in 15mL of bacterial culture media contained in a 50mL conical tube [Abdos P10404] till it reached an OD_{600}=0.8. 2M glycine was added to the culture at one-tenth the culture volume (final concentration 0.2M) 16-24 hours prior to harvesting the cells. The cells were harvested by centrifugation at 3500g for 10 minutes in a centrifuge. The cell pellets were washed three times with 10% glycerol warmed to 37^{o}C, reducing the volume of the wash each time – 10mL, 7mL, 5mL. Care was taken to uniformly homogenize the bacterial pellet

after each. The cells were finally resuspended in 1mL of 10% glycerol warmed to 37ºC and split into 200µL aliquots.

0.5 to 5µg of salt-free DNA in no more than 5µL volume was added to the electrocompetent cells. The cells were transferred to a 0.2cm gap electroporation cuvette [BioRad 165-2086] and were subject to a single pulse of 2.5kV, 25µF, with the pulse-controller resistance set to 1,000Ω resistance. The cells were recovered immediately in 10mL of fresh, warmed bacterial culture media and incubated at 37ºC and 180 rpm shaking for 16-24 hours. The cells were harvested by centrifugation at 3500g for 10 minutes and were resuspended in minimal volume retained after decanting the supernatant. Around 75% of the cell resuspension was spread on warmed 7H11 agar square plates supplemented with OADC and containing suitable antibiotics to select transformants. The plates were incubated at 37ºC, and transformant colonies obtained after 3-4 weeks of incubation.

Electroporation of DNA into Mycobacterium smegmatis

Msm was subcultured from a primary culture in 15mL of bacterial culture media in a 50mL conical tube till it reached an OD600=0.8. The tube was then placed on ice for 1.5 hours. The cells were harvested by centrifugation at 3500g for 10 minutes on a tabletop centrifuge cooled to 4oC. They were then washed three times with ice-cold 10% glycerol, reducing the volume of the wash each time – 10mL, 7mL, 5mL. Care was taken to uniformly homogenize the bacterial pellet after each spin. The cells were resuspended in 1mL of ice-cold 10% glycerol and split into 200µL aliquots, which were then stored at -80ºC for one day before use.

The frozen aliquots of electrocompetent cells were thawed on ice, spun down, and resuspended in 200µL of fresh ice-cold 10% glycerol. 0.5 to 5µg of salt-free DNA in no more than 5µL volume was added to the electrocompetent cells and incubated on ice for 10 minutes. The cells were transferred to an ice-cold 0.2cm gap electroporation cuvette. The cells were subject to one pulse of 2.5kV, 25µF, with the pulse-controller resistance set to 1,000Ω resistance. The cuvette was placed back on ice for 10 minutes, after which the cells were recovered in 10mL of warmed fresh bacterial culture media for 2 hours at 37ºC and 180 rpm.

The cells were then harvested by centrifugation at 3000g for 10 minutes and resuspended in 200µL of bacterial culture media. 50µL and 150µL of the resuspension were spread onto pre-warmed 7H10 agar plates supplemented with ADC and containing suitable antibiotics to select transformants. The plates were incubated at 37^{o}C, and transformant colonies typically obtained after 3 days of incubation.

Transformation of DNA into E. coli using Heat Shock

A 50µL stock of chemically competent DH5α *E. coli* lab strain was thawed on ice for 30 minutes. 100ng of plasmid DNA was added to the cells, and the microcentrifuge tube was flicked gently a few times to mix the components. The mixture was allowed to incubate on ice for 30 minutes. A heat shock at 42 ^{o}C was given for 90s by placing the microcentrifuge tube in a pre-warmed water bath with temperature control [BiOBee Selec TC513]. The tubes were put back on ice for 5 minutes. 950µL of SOC media was added to the tube, and the cells were allowed to recover while shaking in an incubator at 37 ^{o}C and 180 rpm. The tube was centrifuged at 3500g for 5 minutes, and 800µL of the supernatant was aspirated and discarded. The pellet was resuspended in the remaining 200µL of media. 50µL and 150µL of the cell resuspension was plated on pre-warmed LB agar [Himedia GM1151-500G] plates with suitable antibiotics for selection. The plates were incubated at 37 ^{o}C, and transformant colonies typically obtained after an overnight incubation period.

Mammalian Cells and Growth Conditions

Regular Growth Conditions

The murine macrophage cell line RAW 264.7 was cultured in Dulbecco's Modified Eagle's Medium (DMEM) [Cellclone CC3004] supplemented with foetal bovine serum (FBS), sodium pyruvate [Sigma-Aldrich S8636], HEPES solution [Sigma-Aldrich H0887], and L-glutamine [Sigma-Aldrich G8540] at final concentrations of 10% v/v, 1mM, 10mM, 2mM respectively – hereafter referred to as cell culture media. The cells were seeded at a density of 0.2 x 10^{6}/mL of cell culture media in T-25 (10mL culture volume) or T-75 flasks (15-20mL culture volume) [CytoOne CC7682-4875] at 37 ^{o}C and in an atmosphere containing 5% CO_2.

Passage Procedure

RAW 264.7 cells, upon reaching a confluency of 70-80% (usually 48 hours after seeding the previous passage), were detached from the culture flask using a cell scraper [Abdos P21041], collected using a serological pipette and added to a 50mL conical tube with the spent media. The cells were spun down at 1000 rpm (220g) for 5 minutes at room temperature using a tabletop centrifuge [ThermoFisher Scientific Sorvall ST 40R]. The spent media was discarded, and the cell pellet was resuspended in 1mL of pre-warmed fresh cell culture media. 10µL of the resuspension was used to count the number of cells using a haemocytometer. The cells were seeded at a density of 0.2 x 10^6/mL of cell culture media in T-25 (10mL culture volume) or T-75 flasks (15-20mL culture volume) and incubated at 37 ^oC and in an atmosphere containing 5% CO_2.

Revival Procedure

Cell culture media was modified to contain FBS at a final concentration of 20% for the revival procedure. This media is hereafter referred to as revival media.

A stock of RAW 264.7 cells was thawed at room temperature and added to a 50mL conical tube containing 10mL of pre-warmed DMEM. The cells were spun down at 800 rpm (140g) for 5 minutes at room temperature using a tabletop centrifuge [ThermoFisher Scientific Sorvall ST 40R]. The supernatant was discarded, and the cell pellet was resuspended in 1mL of warmed fresh revival media. The cell resuspension was added to a T-25 flask containing 9mL of warmed fresh revival media.

Media was changed the following day with fresh, warmed revival media. Cells were then passaged based on their confluency.

Freezing Procedure

RAW 264.7 cells grown in a T-75 flask were scraped, collected, and counted. The cells were resuspended in a volume of FBS supplemented with DMSO at a final concentration of 10% v/v such that the concentration of cells in the resuspension was between 2 to 3 million per mL. The cells were added to cryovials at a final volume of

1mL per cryovial. The cryovials were placed in a Mr. Frosty™ freezing container in a freezer maintained at -80°C for 24 hours, following which the cryovials were transferred to a liquid nitrogen storage tank wherein the cells were maintained in the vapour phase of liquid nitrogen.

Check for Mycoplasma Contamination

A polymerase chain reaction (PCR)-based test was used to check for the presence of mycoplasma contamination in cultures of RAW 264.7 macrophages.

1.5mL of spent media from the first-day post-revival was aliquoted into a microcentrifuge tube [Axygen MCT-175-C]. It was centrifuged at 3,000 rpm for 5 minutes, and 1mL of the supernatant was added to a fresh microcentrifuge tube. This tube was centrifuged at 11,000 rpm for 10 minutes, and 980µL of the supernatant was aspirated and discarded. 80µL nuclease free water [Ambion AM9906] was added to the remaining 20µL of supernatant. The resuspension was heated at 98 °C for 5 minutes using a heat block [Eppendorf Thermomixer Comfort]. The resuspension was centrifuged at 11,000 rpm for 8 minutes to allow the debris to settle. 30µL of the supernatant was aliquoted and served as the template DNA to be analysed by PCR.

The PCR reaction mix was made as follows:

Table 1: *Reaction components for mycoplasma contamination check by PCR*

Reaction Component	Volume (in µL)
2x GoTaq Green Polymerase	5
10µM Primer mix	1
Template DNA	2
Nuclease Free Water	2
Total	10

The PCR was carried out using a BioRad T100 Thermal Cycler with the following protocol:

Table 2: *Thermal cycler protocol for mycoplasma contamination check by PCR*

Lid temperature – 105 ^{o}C		Reaction Volume – 10µL
Step Number	Temperature	Time
1.	95 ^{o}C	5 minutes
2. Denaturation	94 ^{o}C	30s
3. Annealing	65 ^{o}C	30s
4. Extension	72 ^{o}C	30s
5. Go to Step 2. (34x)		
6.	72 ^{o}C	5 minutes
7.	12 ^{o}C	Infinite hold

Flow Cytometry Analysis of rmgCarvi Fluorescence

Flow cytometry was performed using a BD FACS Aria Fusion flow cytometer equipped with 488nm and 561nm lasers. The FITC (530/30-nm) and PE-Texas Red-mCherry-PI (610/20-nm) emission channels were used to detect the emission wavelengths from the 488nm and 561nm lasers, respectively. The cells were first gated for normalcy and to exclude debris in the SSC-A vs FSC-A plot (**Figure 5A**). The selected cells were then gated for singlet cells in the FSC-H vs FSC-A plot by gating along the main diagonal (**Figure 5B**). The singlet cells were then analysed for their FITC (**Figure 5C**) and PE (**Figure 5D**) fluorescence in their respective plots against SSC-A. The fluorescence thresholds were gated using the non-fluorescent parental wildtype Mtb H37Rv strain, and single fluorescent GFP-expressing and tdTomato-expressing Mtb H37Rv strains. The ratio of the median FITC fluorescence to the median PE fluorescence in the subpopulation of singlet cells positive for PE fluorescence (indicating that these cells express the mCherry fluorophore and are, therefore, rmgCarvi expressing cells) was used as a measure of the intracellular cyclic-AMP concentration. At least 10,000 events per sample were analysed for all experiments.

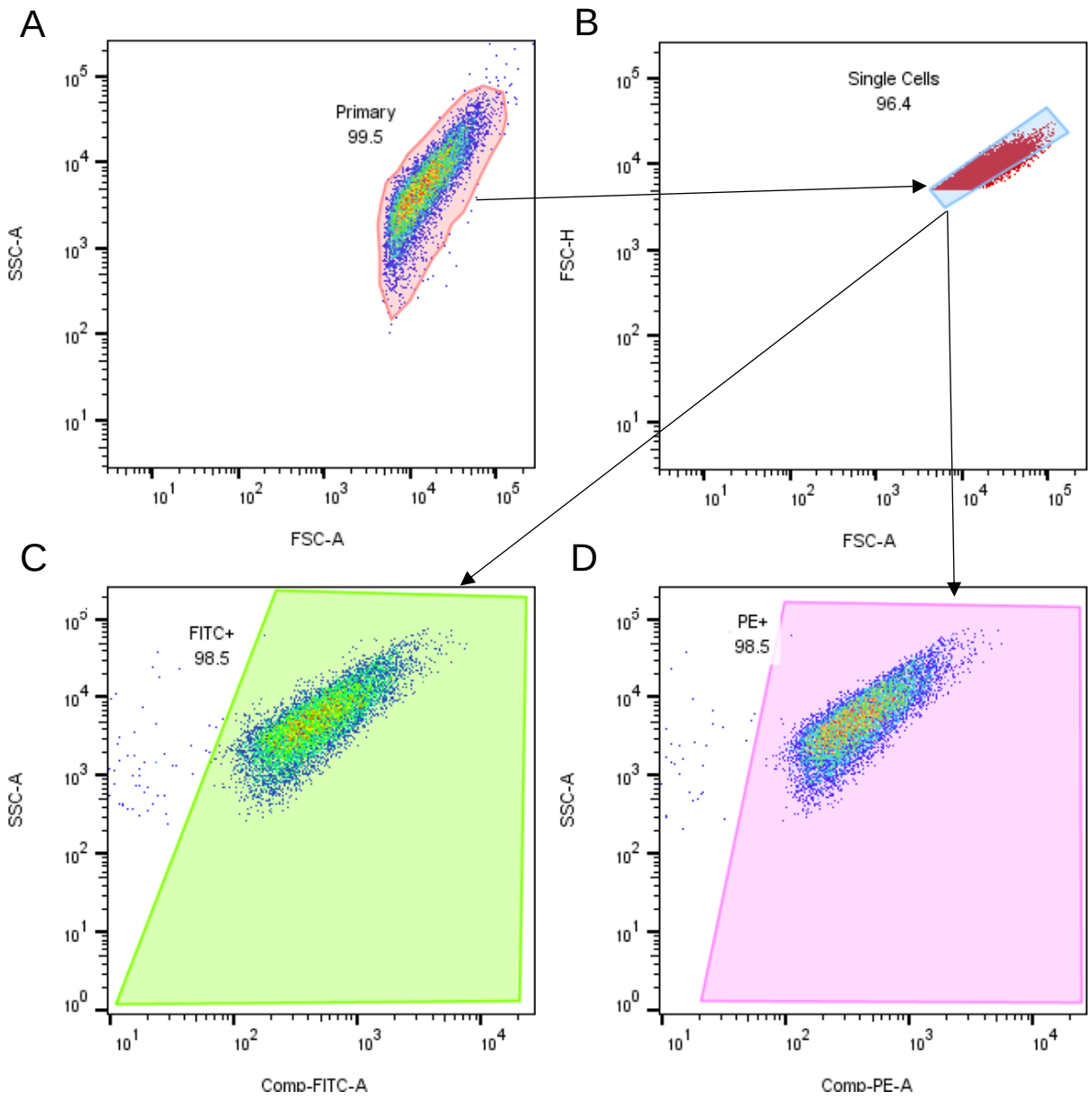

Figure 5: *Gating strategy employed to analyse rmgCarvi expressing Mtb.*

Dormancy and Recovery from Nutrition Starvation in PBST

Mtb expressing rmgCarvi was subcultured from a saturated primary culture in 10mL of bacterial culture media contained in a 50mL conical tube till it reached an OD_{600}=0.6. The cells were harvested by centrifugation at 5000 rpm (4180g) for 5 minutes at room temperature, following which they were washed with 10mL of PBST (phosphate-buffered saline containing tyloxapol at a final concentration of 0.05%). The cells were resuspended in 10mL of PBST and were placed in a shaking incubator maintained at 37 ^{o}C and 180 rpm for 6 weeks.

To rescue the mycobacteria from this state of nutrient starvation-induced dormancy, the cells were harvested by centrifuging at 5000 rpm (4180g) for 5 minutes at room temperature, following which they were resuspended in 1mL of bacterial culture media in a cryovial. The resuspension was subject to three rounds of ultrasonication for 20 seconds, each interspaced by a 20-second break. The cells were then passed through a 26-gauge tuberculin syringe twenty times to make a single-cell suspension. Half the cell resuspension was then added to a 50mL conical tube containing 9.5 mL of bacterial culture media either containing or lacking oleic acid. The culture was sampled at appropriate time points post rescue to measure its OD_{600} using a spectrophotometer and its rmgCarvi fluorescence using a BD FACS Aria Fusion flow cytometer.

Infection of RAW 264.7 Macrophages with Mycobacterium tuberculosis

Seeding RAW 264.7 Macrophages

RAW 264.7 macrophages grown to a confluency of around 70% were scraped and counted as mentioned above. The cells were seeded in a 48-well plate [CytoOne CC7682-7548] at 0.075×10^6 per well in a volume of 300 µL one day prior to infection. The effective number of cells per well at the time of infection is 0.15×10^6.

Activating RAW 264.7 Macrophages with IFN-γ

IFN-γ [PeproTech 315-05] was added to RAW 264.7 macrophages at a concentration of 30 ng/mL at the time of seeding. The cells were seeded at 0.15×10^6 per well of a 48-well plate since IFN-γ activated macrophages do not divide. The same concentration of IFN-γ was added to the cells following their infection with Mtb.

Treating RAW 264.7 Macrophages with Ammonium Chloride

RAW 264.7 macrophages seeded in the wells of a 48-well plates were treated with ammonium chloride [Amresco 0621-1KG] at a final concentration of 10mM at the time of seeding. The same concentration of ammonium chloride was added to the cells following their infection with Mtb.

Treating RAW 264.7 Macrophages with Chloroquine

RAW 264.7 macrophages seeded in the wells of a 48-well plates were treated with chloroquine diphosphate [Sigma C6628-25G] at a final concentration of 10μM at the time of seeding. The same concentration of chloroquine diphosphate was added to the cells following their infection with Mtb.

Infection with Mtb

rmgCarvi expressing Mtb was grown to an $A_{600\ nm}$ of 0.8 in a 50mL conical tube at 37 ^{o}C and 180 rpm shaking. In order to prepare a single-cell suspension of the Mtb, the culture was spun down at 700 rpm (80g) for 5 minutes. The supernatant was collected into a separate 50ml conical tube which was then spun down again at 5000 rpm (4180g) for 5 minutes to harvest the bacteria. The pellet was resuspended in 2mL of cell culture media, and the $A_{600\ nm}$ was measured using a spectrophotometer to estimate the number of bacteria present using the conversion of 0.6 OD_{600} = 1 x 10^8 bacteria. To achieve a multiplicity of infection (MOI) of 10, an appropriate amount of cell culture media was added to the resuspension to achieve a bacterial cell concentration of 30 x 10^6 per mL (1.5 x 10^6 per 50 µL). 50 µL of cell culture media was removed from each well of the 48-well plate, and 50 µL of the bacterial resuspension was added. The cells were placed in an incubator maintained at 37 ^{o}C and an atmosphere containing 5% CO_2. After 3.5 hours of incubation, the cells were administered three washes with PBS to remove any extracellular bacteria and 300 µL of OptiMEM [Gibco 51985-034] supplemented with 5% FBS. This time point corresponds to zero hours of infection. At the required timepoints post-infection, the media in the wells was replaced with PBS, and cells were collected by scraping with a cut micro-pipette tip. The biosensor fluorescence was then measured using flow cytometry (BD FACS Aria Fusion).

Statistical Analysis

Statistical analysis was performed using GraphPad Prism version 8.0.2. All data indicated are mean ± SD. The one sample Wilcox test, one-way ANOVA with Holm-Sidak's multiple comparisons test, and two-way ANOVA with Tukey's multiple comparisons test were used. Differences with $p < 0.05$ were considered significant.

Chapter 3 **Results and Discussion**

1. Investigating Intramycobacterial cyclic-AMP levels during Regular Growth of *Mycobacterium smegmatis* and *Mycobacterium tuberculosis*

The cAMP biosensor rmgCarvi was cloned in the integrative plasmid pND257 and the episomal, multicopy plasmid pMV261. These constructs were transformed into Msm and Mtb in order to monitor intramycobacterial cAMP levels. The episomal version fluoresced with higher intensity in Mtb [data not shown] due to the higher copy number of the plasmid.

Aiming to understand how intramycobacterial cAMP levels varied during regular axenic growth, rmgCarvi fluorescence levels were assayed at regular intervals in growing cultures of *M. smegmatis* and *M. tuberculosis*.

Four biological replicates of *M. smegmatis* expressing rmgCarvi were inoculated from a primary culture at an initial $A_{600\ nm}$ of 0.002 and cultured in either 7H9 media supplemented with either ADC or OADC incubated in an orbital shaker set at 37 ^{o}C and 180 rpm. The cultures were allowed to grow overnight to reach an early exponential stage $A_{600\ nm}$ of around 0.15, following which their optical density was assayed at every doubling time (approximately 2 hours and 45 minutes) using a spectrophotometer, and FITC and PE fluorescence was assayed using a flow cytometer (BDFACS Aria Fusion). The intracellular cAMP levels (measured by taking the ratio of the median FITC fluorescence to the median PE fluorescence for the sample) were seen to increase during the exponential phase of growth, peaking at the late exponential phase (seen at around the 43-hour mark post inoculation) and subsequently reducing as the culture progressed to the stationary phase [**Figures 6A and 6B**]. The intracellular [cAMP] trend was consistent across the four biological replicates and across media conditions that lacked and contained oleic acid. The increased [cAMP] observed at the first time point is likely an artifact of the overnight growth period, reflecting carryover of some stress such as mild hypoxia. The growth curve of the cultures from their time of inoculation is represented in **Figure 6C**. The doubling time of the strain expressing rmgCarvi at 2 hours and 45 minutes was marginally slower than that of the wildtype at 2 hours and 30 minutes. These results

are in general agreement with the only previous analysis of cAMP over growth-phase reported for *M. smegmatis* (Dass *et al.*, 2008).

Three biological replicates of *M. tuberculosis* expressing rmgCarvi were inoculated from a primary culture at an initial $A_{600\ nm}$ of 0.0125 and allowed to grow for two doubling times, following which their optical density was assayed every 24 hours using a spectrophotometer, and FITC and PE fluorescence was assayed by flow cytometry (BDFACS Aria Fusion). This was done to ensure that the fluorescence readings were representative of their current growth phase physiological state and to negate any carryover effects of the stationary culture they were inoculated from. In contrast to what was observed in the case of *M. smegmatis*, intramycobacterial cAMP levels in *M. tuberculosis* were seen to start at a high during the very early stages of exponential growth, following which they reduced and remained relatively constant over the main and late phases of exponential growth from an OD_{600} of 0.2 to 1.5 [**Figures 6D** and **6E**]. The growth curve of the cultures is represented in **Figure 6F**. The trend of intracellular [cAMP] was consistent across the three biological replicates. However, one biological replicate experienced an extended lag phase and was delayed in growth compared to the other two by one division cycle. Therefore, the curves for **Figures 6E** and **6F** represent two biological replicates. To the best of our knowledge, this is the first analysis of cAMP levels within *M. tuberculosis* during axenic growth.

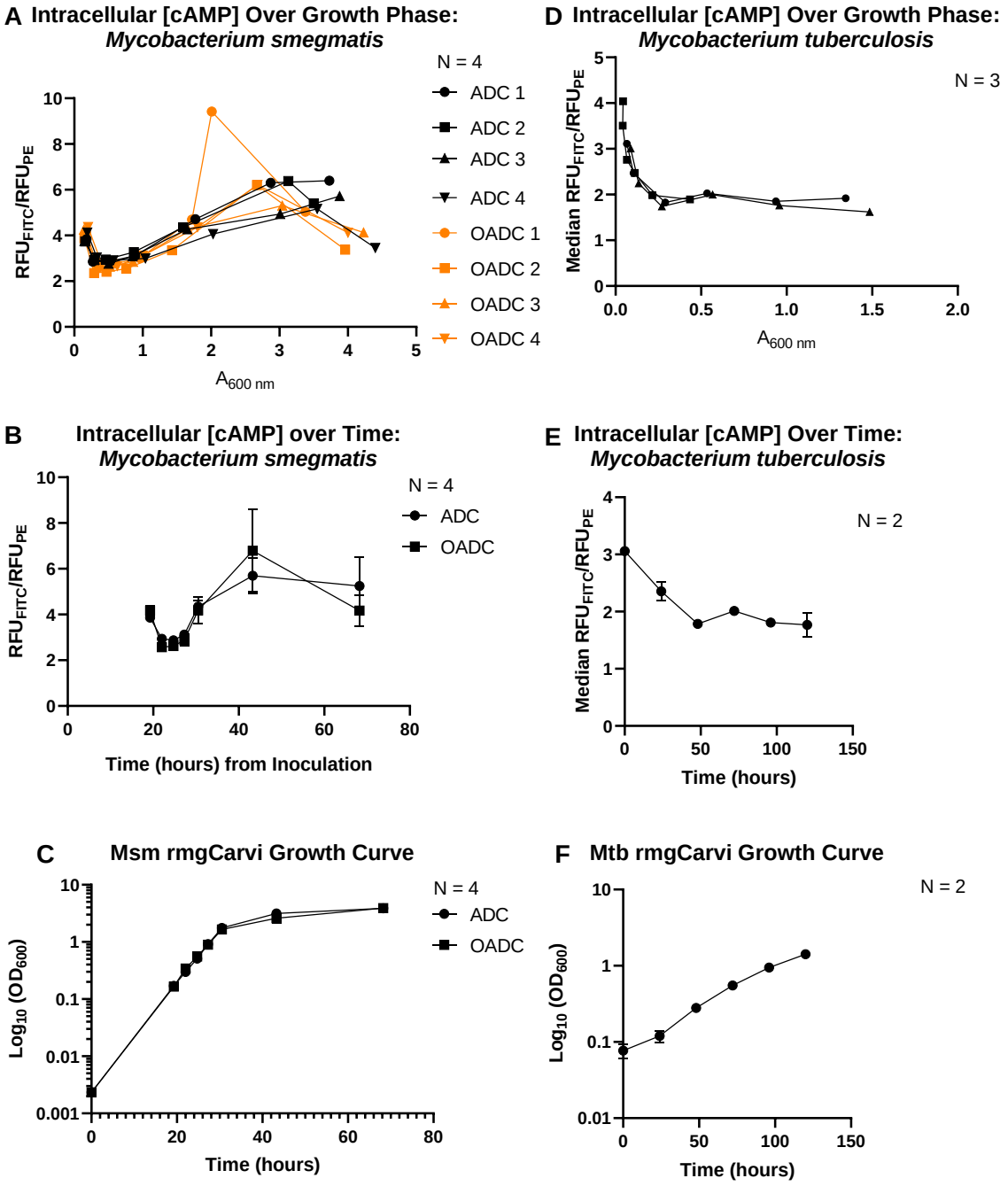

Figure 6: *Intramycobacterial cAMP levels in M. smegmatis and M. tuberculosis during regular growth*. Msm and Mtb strains expressing rmgCarvi were assayed for their FITC and PE fluorescence, measured in relative fluorescence units (RFU), using a flow cytometer and optical density by a spectrophotometer, measured as $A_{600\ nm}$. The ratio of median FITC fluorescence to median PE fluorescence is plotted against $A_{600\ nm}$ or time for Msm (**A**, **B**) and Mtb (**D**, **E**). Growth curves of Msm (**C**) and Mtb (**F**) expressing rmgCarvi.

2. Intramycobacterial Cyclic-AMP Increases upon Resuscitation from Dormancy and Dormant-Like States

cAMP has been shown to be a crucial mediator of free fatty acid-induced resuscitation from dormancy. Dormancy states in Mtb, characterized by the formation of "non-culturable" bacterial states, can be achieved via potassium starvation or upon gradual acidification and static incubation (Shleeva *et al.*, 2013). An increased production of cAMP by Mtb delays the formation of non-culturable bacilli and quicken the resuscitation from dormancy (Shleeva *et al.*, 2017). The fatty acid-inducible adenylyl cyclase *Rv2212* (Abdel Motaal *et al.*, 2006) mediates fatty acid-induced resuscitation from dormancy in a resuscitation-promoting factor (rpf) A-dependent manner in both Msm and Mtb (Shleeva *et al.*, 2013, 2017). *Rv2212* synthesises cAMP in response to the exogenous fatty acids leading to the activation of *Rv3676*, a member of the CRP (cAMP responsive protein of Mtb) family of transcription factors, which directly regulates the expression of rpfA in Mtb in a cAMP-dependent manner (Rickman *et al.*, 2005). Crucially, the stimulatory effect that fatty acids have on *Rv2212* activity is only seen at low ATP concentrations (Abdel Motaal *et al.*, 2006), a hallmark of dormancy. This additionally explains the similarity in cAMP levels between the cultures of Msm grown in the two media conditions during normal growth in **Figures 6A** and **6B**.

Aiming to investigate the cAMP response during resuscitation from dormancy in the presence and absence of free fatty acids, such as oleic acid, in the culture media, we induced the resuscitation from two different states of dormancy in Msm and Mtb. The deep stationary phase of bacterial growth is characterized by low nutrient availability and reduced metabolic activity of the cells (Jaishankar and Srivastava, 2017). This represents a dormancy-mimicking condition wherein cellular ATP levels are low, and *Rv2212*'s fatty acid inducibility could be observed. Msm cultures expressing rmgCarvi were allowed to grow for 7 days at 37 ^{o}C and 180 rpm, resulting in them achieving a deep stationary phase of growth. They were then subcultured into fresh 7H9 media containing either ADC or OADC for 3 hours (around one doubling time) at 37 ^{o}C and 180 rpm and then analysed by flow cytometry.

A 2-fold and 2.8-fold increase in the ratio of median FITC fluorescence to median PE fluorescence was observed upon rescue from deep stationary phase in 7H9 containing ADC and OADC, respectively [**Figure 7A**]. Additionally, there was less than a 5%

change in the median PE fluorescence upon rescue from deep stationary in both media conditions within three hours [**Supplementary Figures 1A** and **1B**]. The PE fluorescence from the mCherry fluorophore is a proxy for the rmgCarvi protein levels in the cell since it is constitutively fluorescent. This indicates that after 3 hours of rescue from deep stationary phase, there is a negligible change in the rmgCarvi steady-state protein levels but a dramatic and statistically significant increase in ratio of FITC to PE fluorescence in an oleic acid-dependent manner. Put together, this data robustly indicates a significant increase in intramycobacterial cAMP levels upon rescue from deep stationary phase in an oleic acid-dependent manner.

Nutrient starvation represents a form of *in vitro* dormancy in *Mycobacterium tuberculosis* (Gold and Nathan, 2017) characterized by an altered gene and protein expression profile (Betts *et al.*, 2002), translation regulation (Sawyer *et al.*, 2021) and increased drug tolerance to frontline anti-TB drugs (Betts *et al.*, 2002; Xie *et al.*, 2005; Block *et al.*, 2023). To induce this form of dormancy, exponential cultures of rmgCarvi expressing Mtb were washed with PBST (phosphate-buffered saline containing tyloxapol at a final concentration of 0.05%) to remove any remaining nutrients in the culture, following which they were resuspended in fresh PBST and allowed to incubate at 37 ^{o}C and 180 rpm for 6 weeks. This represents an aerobic form of nutrient starvation-induced dormancy due to the shaking of the culture. Within one week of nutrient starvation, the cultures of Mtb had formed biofilms and aggregated into clumps. Following six weeks of nutrient starvation, the cultures were rescued into fresh culture media supplemented either with ADC or OADC. Their optical density and rmgCarvi fluorescence were assayed using a spectrophotometer and flow cytometer, respectively.

A rapid increase in intramycobacterial cAMP levels was observed upon resuscitation from nutrient starvation-induced dormancy within 10 minutes – representing the time taken from rescuing the cultures to assaying them using flow cytometry. A dramatic increase in cAMP levels of over 4-fold was observed within 3 hours of resuscitation from dormancy in the form of a cAMP-spike that lasted at least until 24 hours post-rescue. This increase was independent of the presence of exogenous free fatty acids. An oleic-acid-dependent increase in intramycobacterial cAMP levels was observed, however, this difference was confined to the 3-hour time point alone. The rescued

cultures continued to maintain a significantly higher level of intramycobacterial cAMP relative to cultures in exponential growth until 120 hours post-rescue [**Figure 7B**]. The growth dynamics of the cultures rescued from nutrient starvation-induced dormancy were characterized by a lag phase of 24 hours, following which they displayed a typical doubling time of about 24 hours [**Figure 7C**]. Along similar lines to what was observed in the case of *M. smegmatis'* recovery from the deep stationary phase, the PE fluorescence measured from the constitutively fluorescent mCherry fluorophore saw a minor increase of only 16% within one-day post-resuscitation, following which a linear increase was observed over the remainder of the resuscitation period [**Supplementary Figure 1C**].

These results are in good agreement with published data (Shleeva *et al.*, 2013, 2017) and point towards a model [**Figure 7D**] wherein exogenous free fatty acids, like oleic acid, stimulate *Rv2212*'s adenylate cyclase activity in the low ATP paradigm of dormancy. The increased cytosolic cAMP binds to and activates CRP, leading to the increased expression of rpfA, thereby resulting in resuscitation from dormancy. However, our data reveals two additional components to this existing paradigm. 1) There is a dramatic increase in intramycobacterial cAMP upon resuscitation from dormancy even in the absence of any exogenous free fatty acids. 2) The timescale of this cAMP spike upon resuscitation in the absence of exogenous free fatty acids is of the order of a few minutes, if not even faster – quicker than the kinetics of a transcriptional response to meaningfully alter steady-state protein levels (Golding *et al.*, 2005; Mitosch *et al.*, 2019). There likely exists an unidentified signalling pathway that induces cAMP rapidly in response to glucose and/or glycerol (both of which are present in 7H9 supplemented with ADC), with a two-component system being a prime candidate of being the mediator due to the rapid kinetics of their activity (Yamamoto *et al.*, 2005). Additionally, CRP has been shown to be implicated in the cAMP response to *in vitro* salt stress (Rebollo-Ramirez and Larrouy-Maumus, 2019). Although the exact mechanism of this signalling is currently unknown, CRP has been strongly predicted to bind to the promoter region of the cAMP phosphodiesterase Rv0805 (Bai et al., 2005), offering a potential explanation for its role in modulating cAMP levels. Nevertheless, this does indicate the possible presence of a positive feedback loop of cAMP production upon resuscitation from dormancy (and most other cAMP-inducing stimuli) mediated by CRP.

At first glance, it might seem that a dramatic increase in cAMP production during resuscitation from dormancy is counterintuitive since it is a sink for usable ATP, a highly constrained resource in the cell when it is dormant. However, Mtb is able to leverage this increased cytosolic cAMP pool via its signalling properties to facilitate its recovery from dormancy (Shleeva *et al.*, 2017). Additionally, It is known that increased cAMP levels correlate with an increased growth rate in Mtb (Thomson *et al.*, 2022). Further, unpublished data from our lab has revealed the existence of a cAMP pulse immediately preceding and following cleavage furrow formation as Mtb divides, indicating strong ties between cAMP and cell cycle control and increased growth rate, as has shown to be the case in *E. coli* (D'Ari *et al.*, 1988).

A cAMP Increase in *Mycobacterium smegmatis* during Rescue from Deep Stationary Phase

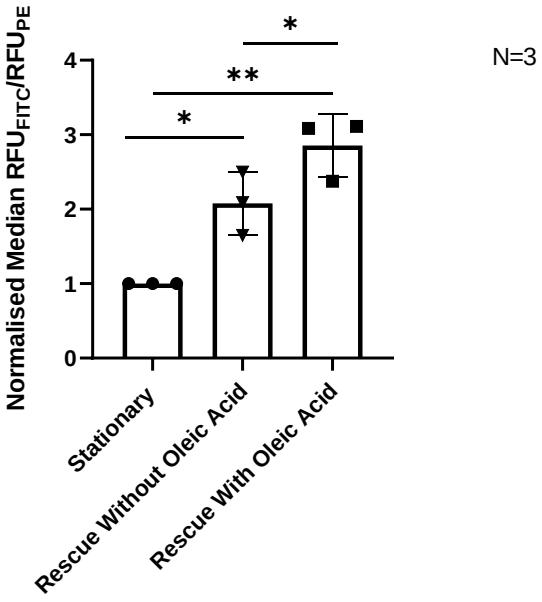

B cAMP Increase in *Mycobacterium tuberculosis* Upon Resuscitation from Nutrition Starvation-Induced Dormancy

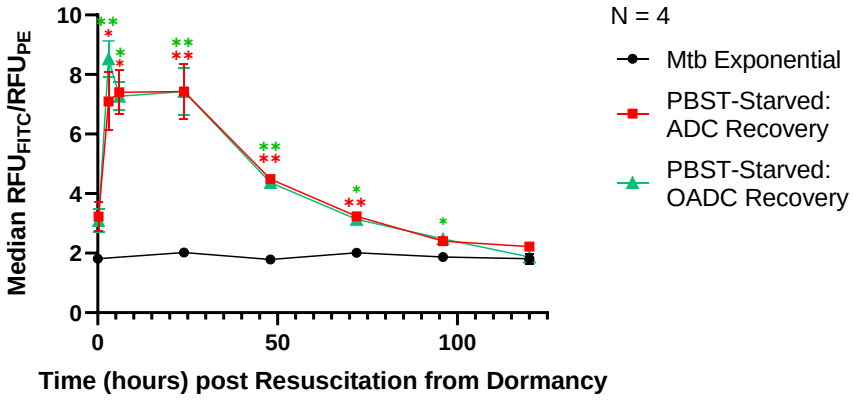

C *Mycobacterium tuberculosis* Growth Upon Resuscitation from Nutrition Starvation-Induced Dormancy

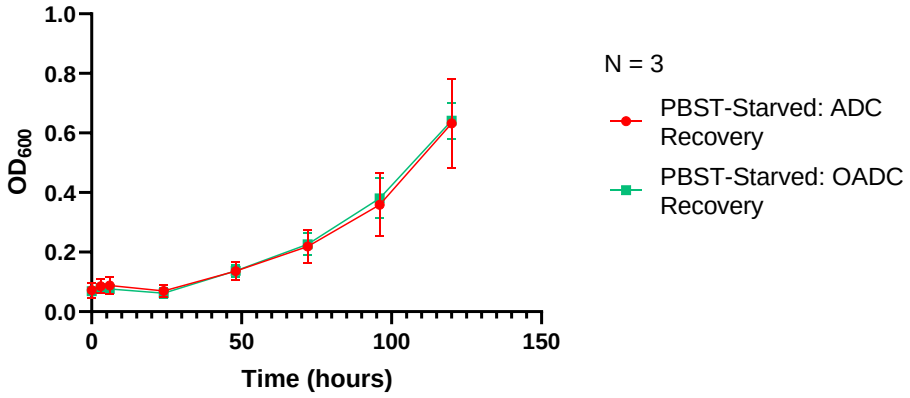

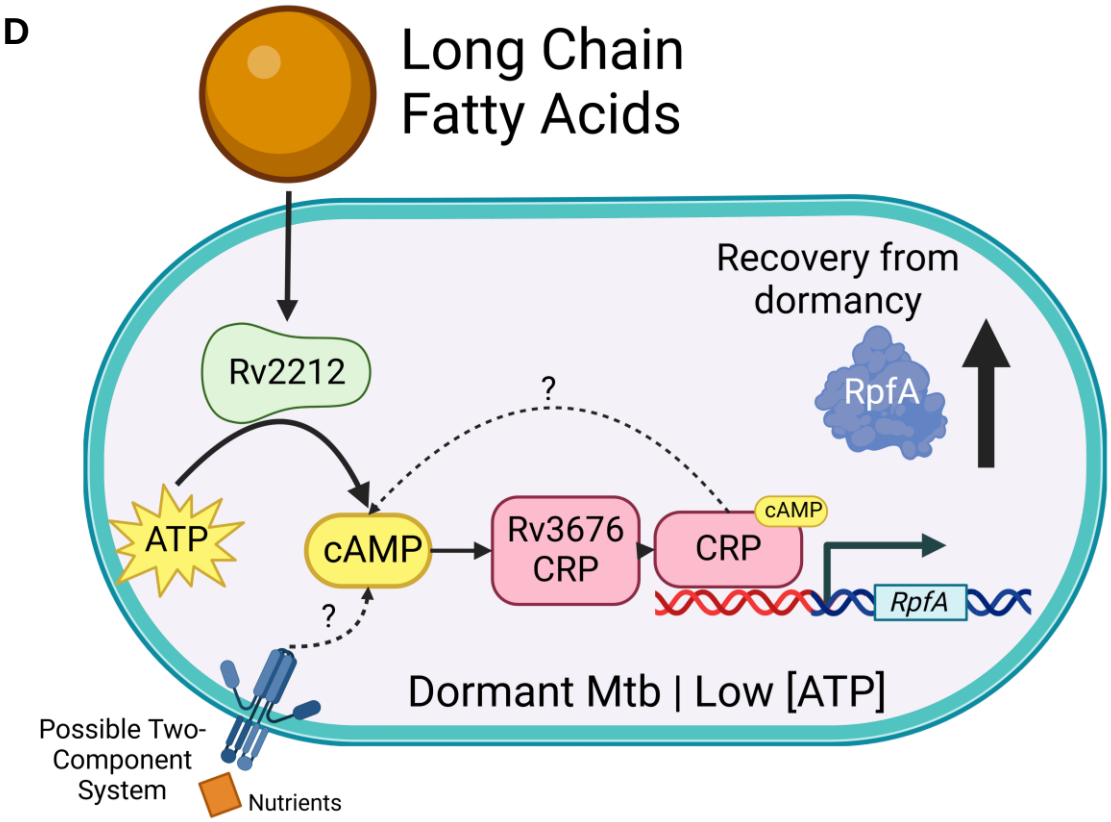

Figure 7: *Intramycobacterial cyclic-AMP increases upon resuscitation from dormancy and non-culturable bacterial state.* **(A)** rmgCarvi expressing cultures of Msm were incubated in a shaker for 7 days to reach deep stationary phase, following which they were rescued into fresh culture media supplemented with ADC or OADC and their biosensor fluorescence was measured 3 hours post rescue. The ordinate reports the ratio of the median FITC fluorescence to the median PE fluorescence for each culture relative to that in deep stationary phase. The error bars represent the standard deviation. Statistical analysis was conducted using a one-way ANOVA with Holm-Sidak's multiple comparison test. *, $p<0.0332$. **(B-C)** rmgCarvi expressing cultures of Mtb were starved of all nutrients and incubated with shaking for 6 weeks in PBST, following which they were rescued into fresh culture media supplemented with ADC or OADC. Their biosensor fluorescence **(B)** and optical density **(C)** was measured at the denoted timepoints. The error bars represent the standard deviation. Statistical analysis was conducted using a non-spherical two-way ANOVA with Tukey's multiple comparisons test. *, $p<0.0332$; **, $p<0.0021$. The green and red asterisks denote a significant difference between the 'PBST-Starved: OADC Recovery' and the 'PBST-Starved: ADC Recovery' conditions with the 'Mtb Exponential' condition respectively. **(D)** Model of fatty-acid-induced and independent resuscitation from dormancy mediated by cAMP. Created in https://BioRender.com.

3. *Mycobacterium tuberculosis'* cAMP Response to Physiologically Relevant Stresses *In vitro*

Upon its engulfment by macrophages, *Mycobacterium tuberculosis* resides in early phagosomes that are characterized by a pH of 5 to 5.5 (Yates *et al.*, 2005) and a salt concentration of around 250mM (Larrouy-Maumus *et al.*, 2016). While it is known that both these environmental stresses induce an elevated production of cAMP in Mtb *in vitro* (Rebollo-Ramirez and Larrouy-Maumus, 2019; Khan *et al.*, 2024), the temporality of this cAMP response and its nature in response to both stresses in combination is unknown. We set out to investigate these properties by leveraging the rmgCarvi biosensor.

Three biological replicates of rmgCarvi expressing Mtb were grown to an exponential phase $A_{600\ nm}$ of 0.8 and inoculated either in culture media containing a salt concentration of 250mM, or maintained at an acidic pH of 5.5, or a combination of the two. The rmgCarvi fluorescence was then measured by flow cytometry. The results are shown in **Figure 8**.

Within 15 minutes of exposure to salt stress (representing the time taken from exposing the bacilli to the stress to assaying them using flow cytometry), either in combination with the acidic pH or alone, a robust elevation in intramycobacterial [cAMP] was observed relative to the parental culture. However, this was not the case for cultures exposed to acidic stress alone. The acid and salt stress, when present alone, resulted in a strong increase in intramycobacterial [cAMP] by the 3-hour mark. However, when both stresses were present in combination, intramycobacterial cAMP levels reduced from their levels at the early induction time point and were close to that under the acidic stress alone. At the 6-hour time point, there was a concerted decrease in intramycobacterial cAMP levels across all treatment conditions. This was followed by an increase in intramycobacterial cAMP levels at the 24-hour time point and a reduction at the 48-hour time point.

The presence of a rapid cAMP response to salt stress and the lack of one in response to acidic stress at the 15-minute timepoint likely indicates the presence of a different modality of cAMP induction in response to these stresses. The eukaryotic-like serine-threonine kinase PknD has been implicated in Mtb's adaptation to salt stress (Hatzios

et al., 2013), including its cAMP response at 6 hours post-exposure to 250mM salt stress (Rebollo-Ramirez and Larrouy-Maumus, 2019). PknD is a likely candidate for conferring this rapid cAMP response to salt stress. However, the underlying molecular mechanisms by which it influences cAMP levels are yet to be identified.

The molecular mechanisms behind the cAMP response to individual acid stress at the 3-hour timepoint have been robustly elucidated in the literature. The PhoPR two-component system has been shown to be responsible for sensing and responding to acidic stress (Abramovitch *et al.*, 2011; Tan *et al.*, 2013; Bansal *et al.*, 2017) and inducing cAMP levels in response to acidic stress by transcriptionally repressing the cAMP phosphodiesterase *Rv0805* (Khan *et al.*, 2024). While CRP has been shown to be implicated in the cAMP response to *in vitro* salt stress (Rebollo-Ramirez and Larrouy-Maumus, 2019), mechanistic explanations are not yet conclusive. CRP has been shown to alter the expression levels of the adenylate cyclases *Rv0386, Rv0891c, Rv1318c, Rv1320c, Rv1625c*, and *Rv3645* (Cortes *et al.*, 2013; Kahramanoglou *et al.*, 2014; Rebollo-Ramirez and Larrouy-Maumus, 2019). Additionally, CRP has been predicted to regulate the expression of the PDE *Rv0805* (Bai *et al.*, 2005). While a transcriptional response regulating cAMP levels in response to salt stress does fit the timescale of regulation lasting up to 24 hours post-exposure to the stress, a clear mechanistic link is yet lacking.

There are two likely explanations for the reduction in intramycobacterial cAMP levels observed in response to the combination of acid and salt stresses at the 3-hour timepoint relative to the early induction observed. 1) cAMP is actively degraded, or 2) cAMP is exported out of the cell. Mtb is known to respond to acidic pH and salt stress in a synergistic manner (Tan *et al.*, 2013). PhoP, when phosphorylated by PhoR (which occurs upon encountering acidic stress amongst other cues), has been shown to promote the recruitment of and binding of CRP (which need not be bound to cAMP) at the promoter regions of crucial virulence-determining genes (Khan *et al.*, 2022). Given that activated PhoP has been shown to bind to the promoter region of *rv0805* and repress its transcription (Khan *et al.*, 2024), and CRP has been strongly predicted to bind to the promoter region of *rv0805* (Bai *et al.*, 2005), it is likely that the same principle of synergism applies to the transcriptional repression of the cAMP phosphodiesterase *rv0805.* Therefore, in response to a combination of acid and salt

stresses, a very high level of cAMP is likely to build up. However, given the highly complex nature of cAMP signalling in Mtb, an unbalanced level of cytosolic cAMP likely will disrupt multiple cAMP-dependent signalling processes, causing the expulsion of cAMP out of the cell to keep cytosolic cAMP levels in check. A known example of Mtb regulating its cAMP levels to intermediate levels has been shown in the presence of cholesterol and fatty acids – both important, physiologically relevant carbon sources (Pandey and Sassetti, 2008; Russell *et al.*, 2009; Lee *et al.*, 2013; Lerner *et al.*, 2017). Low levels of intramycobacterial cAMP lead to increased fatty acid uptake and toxicity (Nazarova *et al.*, 2019; Wong *et al.*, 2023), whereas Mtb cannot metabolise cholesterol in conditions of high intramycobacterial cAMP (Wilburn *et al.*, 2022). Therefore, it is more likely that the Mtb produces a very large amount of cAMP in response to these physiologically relevant stresses *in vitro* and exports the cAMP out of the cell.

An explanation for the observed reduction in intramycobacterial cAMP levels at the 6-hour timepoint across all treatments will be given in the next section.

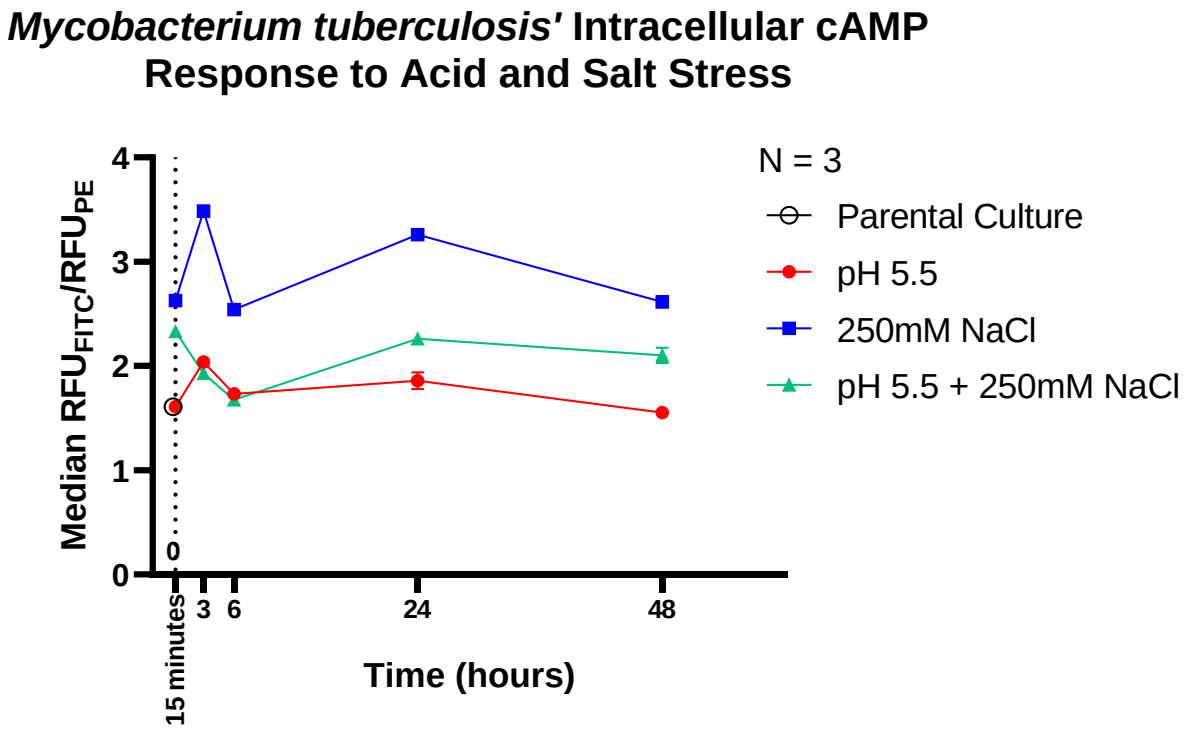

Figure 8: *Mycobacterium tuberculosis' cAMP response to physiologically relevant stresses in vitro.* Three biologically independent cultures of rmgCarvi expressing Mtb were cultures to an exponential phase $A_{600\ nm}$ of 0.8 following which they were exposed to either an acidic pH of

5.5, salt stress of 250mM or both in combination in their culture media. rmgCarvi fluorescence was assayed by flow cytometry.

4. Temporal Dynamics of Intramycobacterial cAMP During Infection in RAW 264.7 Macrophages

Upon infection of *Mycobacterium tuberculosis* in host macrophages, a dramatic change in the cAMP landscape in both cells have been reported, as discussed in the introduction. Aiming to reproduce these results and delineate the temporal dynamics of cAMP crosstalk during infection of Mtb in the RAW 264.7 murine macrophage cell line, infections were carried out using rmgCarvi expressing Mtb and infected cells were assayed at appropriate intervals using flow cytometry.

Validating the previously reported results in (Bai *et al.*, 2009), a consistent increase in intramycobacterial cAMP levels was observed upon infection in RAW 264.7 macrophages relative to axenic Mtb (**Figure 9A**). Intramycobacterial cAMP levels were assayed at 3-, 6- and 24-hours post-infection to facilitate an understanding of how cAMP levels changed within Mtb over infection time in macrophages. Intramycobacterial cAMP levels were observed to undergo a very reproducible reduction at 3 hours post-infection, and with levels stabilizing at the 6h and 24h time points (**Figures 9B** and **9C**).

The observed decrease in intramycobacterial cAMP levels at 3-hour post-infection timepoint correlates precisely with the reported cAMP burst into the host macrophage (J774 and THP-1 cell lines) (Agarwal *et al.*, 2009). While our data does not conclusively show that the reduction in intramycobacterial cAMP levels is due to a cAMP burst into the host macrophage since we have not assayed intramacrophage cAMP levels at these time points, it is the first report that quantifies intramycobacterial cAMP levels during infection in a dynamic manner. In contrast to the findings in Agarwal *et al.,* 2009, a recent study investigating cAMP during Mtb infection, did not observe the presence of a cAMP burst upon infection of Mtb into human monocyte-derived macrophages up to 24-hours post infection (Leopold Wager *et al.*, 2023). A combination of different host cell types, infective dose of Mtb and the sensitivities of the cAMP detection mechanisms could potentially explain the opposing results.

A **Normalized rmgCarvi Fluorescence Upon Infection**

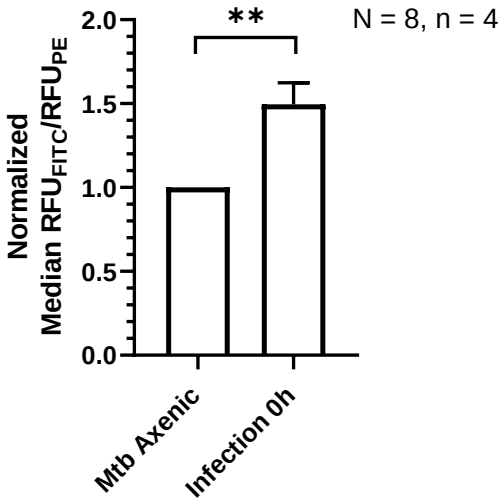

B **rmgCarvi Fluorescence Over Infection Time**

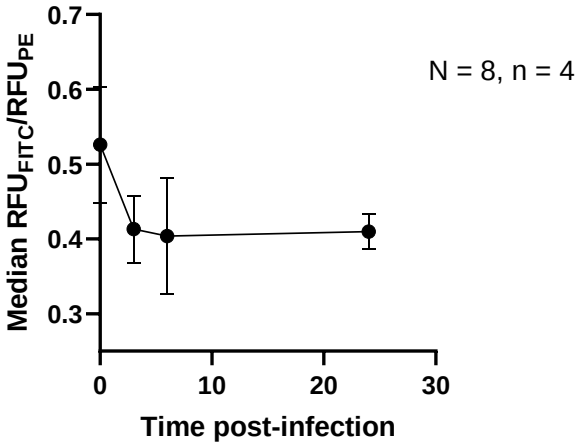

C **Normalized rmgCarvi Fluorescence Over Infection Time**

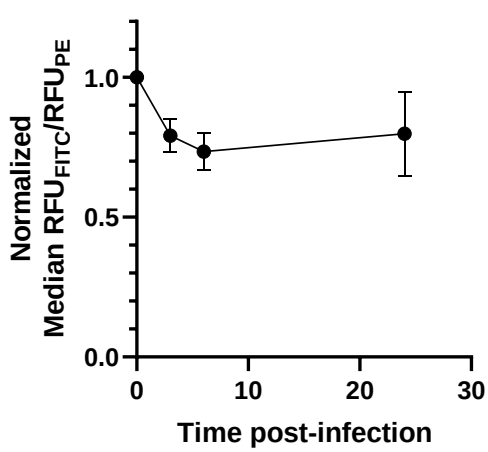

Figure 9: *Temporal dynamics of intramycobacterial cAMP during infection in RAW 264.7 macrophages.* Intramycobacterial cAMP levels were assayed using rmgCarvi fluorescence after the incubation period of macrophage infection (**A**) and over infection time (**B,** represents the ratio of median FITC to median PE fluorescence; **C**, represents the same value normalized to that at the 0-hour post-infection timepoint). The error bars represent the standard deviation. Statistical analysis was carried out using the one sample Wilcox test. **, $p < 0.01$.

4.1. *Isoniazid Treatment Does not Appreciably Affect Intramycobacterial cAMP During Infection*

A recent study found cAMP to be implicated in conferring resistance to a number of antibiotics *in vitro*, conditional on the presence of exogenous free fatty acids. Interestingly, there was no consistent correlation between cAMP induction upon treatment with the antibiotic *in vitro* and resistance conferred by cAMP to the antibiotic (Wong *et al.*, 2023). However, the study did not assess these phenomena upon infection. We set out to investigate the influence of the frontline anti-tubercular drug isoniazid (INH) on cAMP levels *in vitro* and upon infection in RAW 264.7 macrophages.

A minor, but statistically non-significant, reduction in intramycobacterial cAMP levels was observed upon infection in macrophages and treatment with three times the minimum inhibitory concentration (MIC) of INH (0.4µg/mL) in comparison to the no drug treatment (**Figure 10A**). The intramycobacterial cAMP profile over infection time with INH treatment followed the no-drug treatment closely, and no difference was observed in the magnitude or duration of the cAMP burst (**Figures 10B and 10C**).

Upon treating rmgCarvi expressing Mtb with the same concentration of INH *in vitro*, a robust 1.6-fold increase in intramycobacterial cAMP levels was observed 3-hours post-treatment. Following a reduction at 6 hours, INH continued to induce an elevated production in cAMP in Mtb up to 24 hours of treatment (**Figure 10D**).

A **Normalized rmgCarvi Fluorescence Upon Infection**

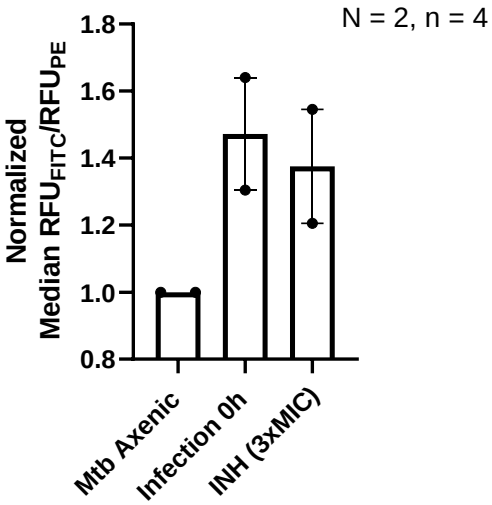

B **rmgCarvi Fluorescence Over Infection Time**

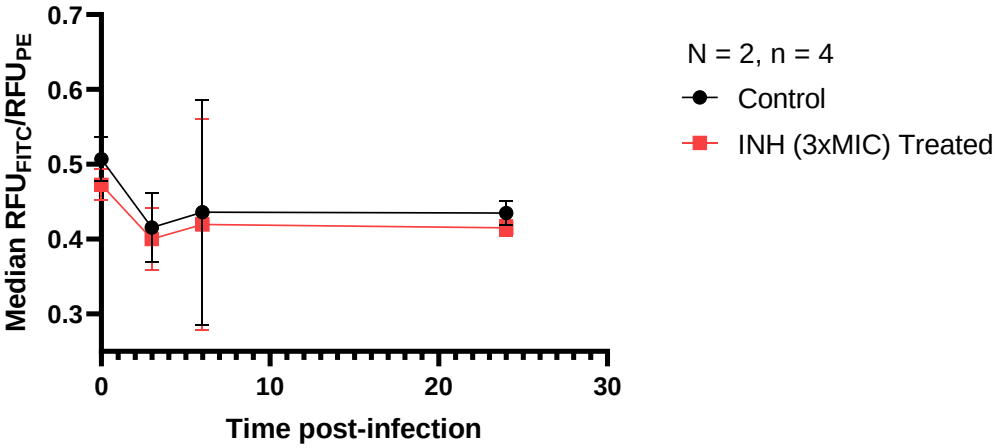

C **Normalized rmgCarvi Fluorescence Over Infection Time**

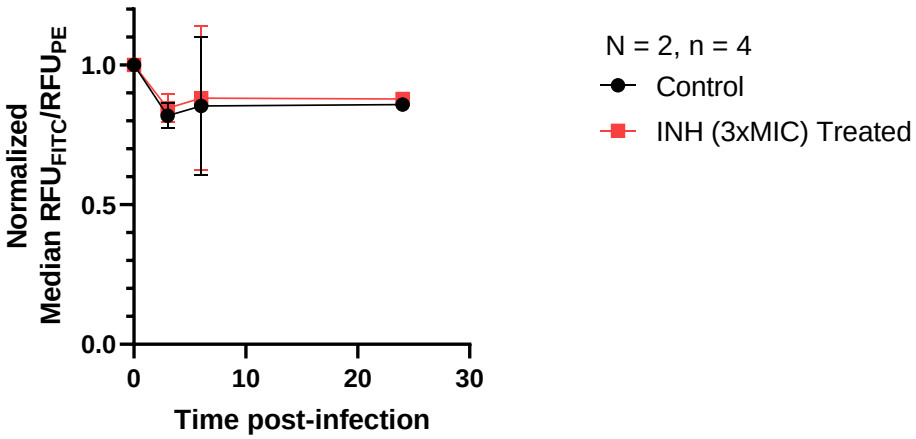

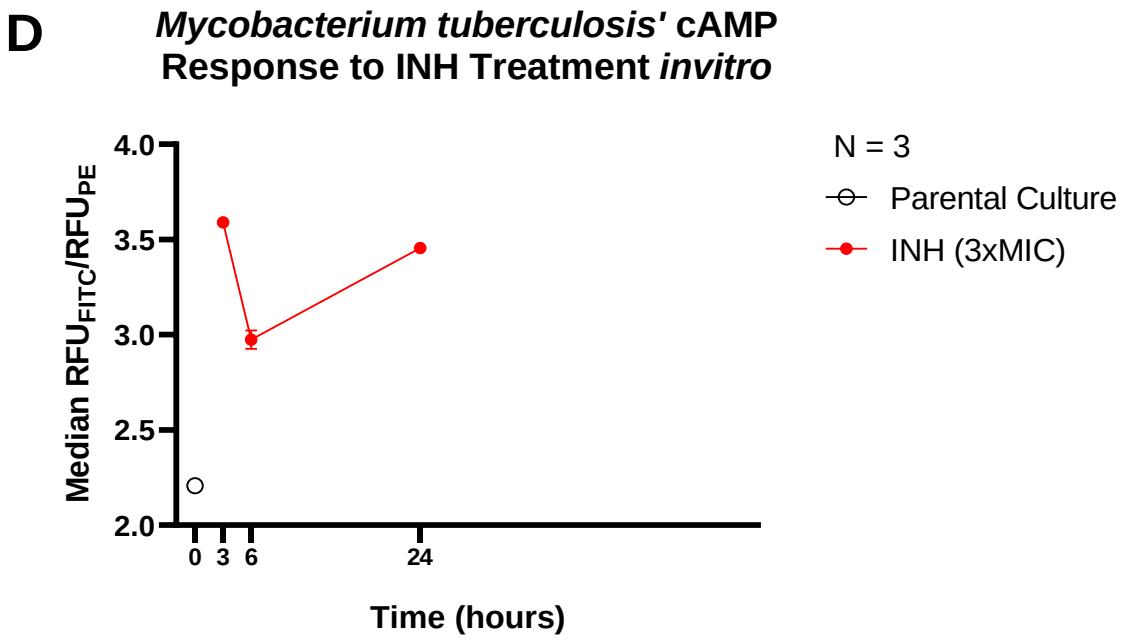

Figure 10: *Isoniazid treatment does not appreciably affect intramycobacterial cAMP during infection.* Intramycobacterial cAMP levels were assayed using rmgCarvi fluorescence after the incubation period of macrophage infection (**A**) and over infection time (**B,** represents the ratio of median FITC to median PE fluorescence; **C**, represents the same value normalized to that at the 0-hour post-infection timepoint). **(D)** The effect of INH treatment on intramycobacterial cAMP levels *in vitro*. The error bars represent the standard deviation.

4.2. *Infection in IFN-γ Activated Macrophages Induces an Elevated cAMP Production and Burst*

Interferon (IFN)-γ is a proinflammatory cytokine that promotes improved microbicidal activity of macrophages by promoting increased receptor-mediated phagocytosis, production of reactive oxygen species (ROS), reactive nitrogen intermediates (RNIs), phagosomal acidification, lysosomal enzyme production and autophagic response (Schroder *et al.*, 2004; Philips and Ernst, 2012; Kak *et al.*, 2018). Further, IFN-γ has been shown to be essential for the control of tuberculosis infection in both mice and humans (Jouanguy *et al.*, 1999). In line with the model discussed in the introduction and illustrated in **Figure 2**, we hypothesized that infection of Mtb in IFN-γ-activated macrophages would result in an increase in intramycobacterial cAMP production and a cAMP burst of a greater magnitude to combat the increased autophagic response.

A significant increase in intramycobacterial cAMP levels was observed upon infection in IFN-γ-activated-macrophages compared to in naïve macrophages (**Figure 11A**). Further, a cAMP burst of increased magnitude was observed at the 3-hour post-infection timepoint when Mtb was internalized by IFN-γ-activated-macrophages relative to naïve macrophages (**Figures 11B** and **11C**). These results are in line with our hypothesis and provide validation to the model (**Figure 2**) discussed in the introduction.

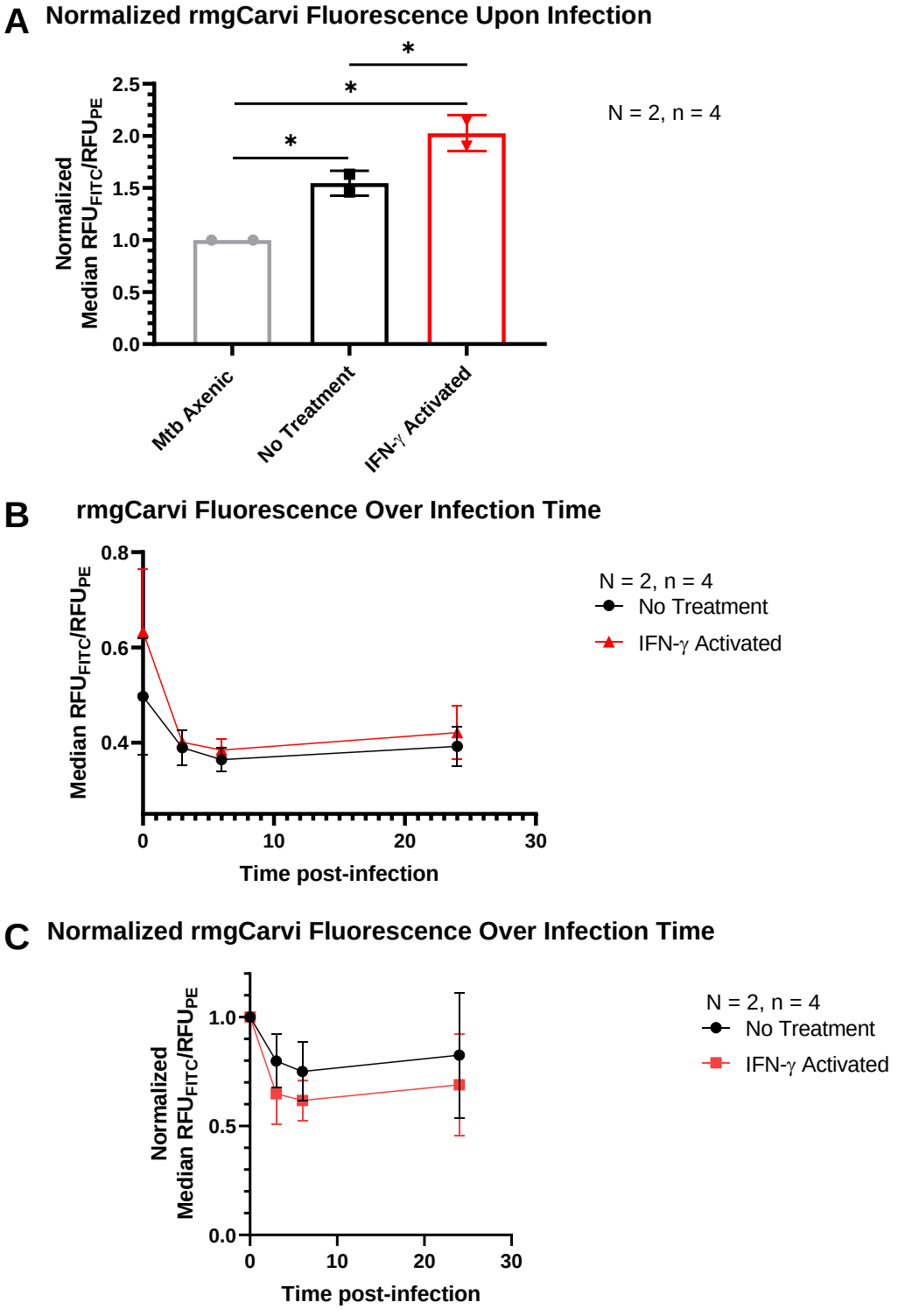

Figure 11: *Infection in IFN-γ activated macrophages induces an elevated cAMP production and burst.* Intramycobacterial cAMP levels were assayed using rmgCarvi fluorescence after the incubation period of macrophage infection (**A**) and over infection time (**B,** represents the ratio of median FITC to median PE fluorescence; **C**, represents the same value normalized to

that at the 0-hour post-infection timepoint). The error bars represent the standard deviation. Statistical analysis was conducted using a one-way ANOVA with Holm-Sidak's multiple comparison test. *, $p<0.0332$.

4.3. *The Acidic Environment of the Early Phagosome is not the Primary Driver of Elevated Intramycobacterial cAMP Upon Infection*

After observing the robust and reproducible increase in intramycobacterial cAMP levels upon infection, we speculated that there are likely four possible inducers of the phenomenon – 1) the acidic pH of the early endosome (Yates *et al.*, 2005), 2) the increased salt concentration of the early endosome (Larrouy-Maumus *et al.*, 2016), 3) the altered nutrient sources available to Mtb in the macrophage (Pandey and Sassetti, 2008; Russell *et al.*, 2009; Lee *et al.*, 2013; Lerner *et al.*, 2017), and 4) antimicrobial peptides and other host-induced stimulators of cAMP. Since cAMP has been implicated in preventing phagosome maturation (Kalamidas *et al.*, 2006; Leopold Wager *et al.*, 2023), a phenomenon that is intimately linked with increased acidification (Yates *et al.*, 2005), which in turn has been shown to regulate cAMP levels (Khan *et al.*, 2024), we hypothesize that the acidic pH of the early endosome was most likely to be the driver of the increase in cAMP production in Mtb upon infection. We adopted two strategies in order to test this hypothesis. The first involved infecting Mtb in macrophages that had been pre-treated with known phagosomal de-acidification agents such as ammonium chloride (Hart *et al.*, 1983; Hart and Young, 1991; Conte *et al.*, 1996) and chloroquine (Al-Bari, 2017; Mauthe *et al.*, 2018; Coban, 2020) overnight. It has been shown that Mtb infected in macrophages treated with chloroquine (CQ) prior to infection for one hour experience an environment of neutral pH in the phagosome 6 hours post-internalization, identically to the case of macrophages treated with the V-ATPase inhibitor Bafilomycin A1 (Mishra *et al.*, 2019). The second involved pre-acclimatizing Mtb to a pH of 5.5 for 3 hours before infection.

A robust 1.5-fold increase in cAMP levels was observed upon exposing axenic Mtb to a pH of 5.5 for 3 hours, confirming the expected induction of the treatment prior to infection (**Figure 12A**). Interestingly, there was no statistically significant difference in intramycobacterial cAMP levels upon infection in macrophages that had been treated with ammonium chloride or chloroquine, or in Mtb that had been pre-

acclimatized to a pH of 5.5 (and therefore had elevated intramycobacterial cAMP upon infection) relative to the no-treatment condition (**Figures 12A** and **12B**). The temporal dynamics or magnitude of the cAMP burst also did not change significantly with any of the treatment cases (**Figures 12B**-**C** and **12E**-**F**).

In combination, these results indicate that the acidic pH of the early phagosome is likely not the primary driver for the increased production of cAMP in Mtb upon infection. The Mtb that had been pre-acclimatized to the acidic pH likely did not find a requirement to produce any more cAMP upon infection due to its already elevated intramycobacterial cAMP level. In the absence of an acidic environment in the phagosomes containing Mtb (upon treating macrophages with either ammonium chloride or chloroquine), the other possible drivers of cAMP production including the elevated salt concentration of the phagosome, altered nutrient sources, antimicrobial peptides and other factors could all be at play. Given the highly interlinked and complex nature of cAMP signalling in Mtb, it is unlikely that a single inducer would be responsible for an induction of cAMP upon infection in macrophages, Mtb's most common niche over evolutionary history.

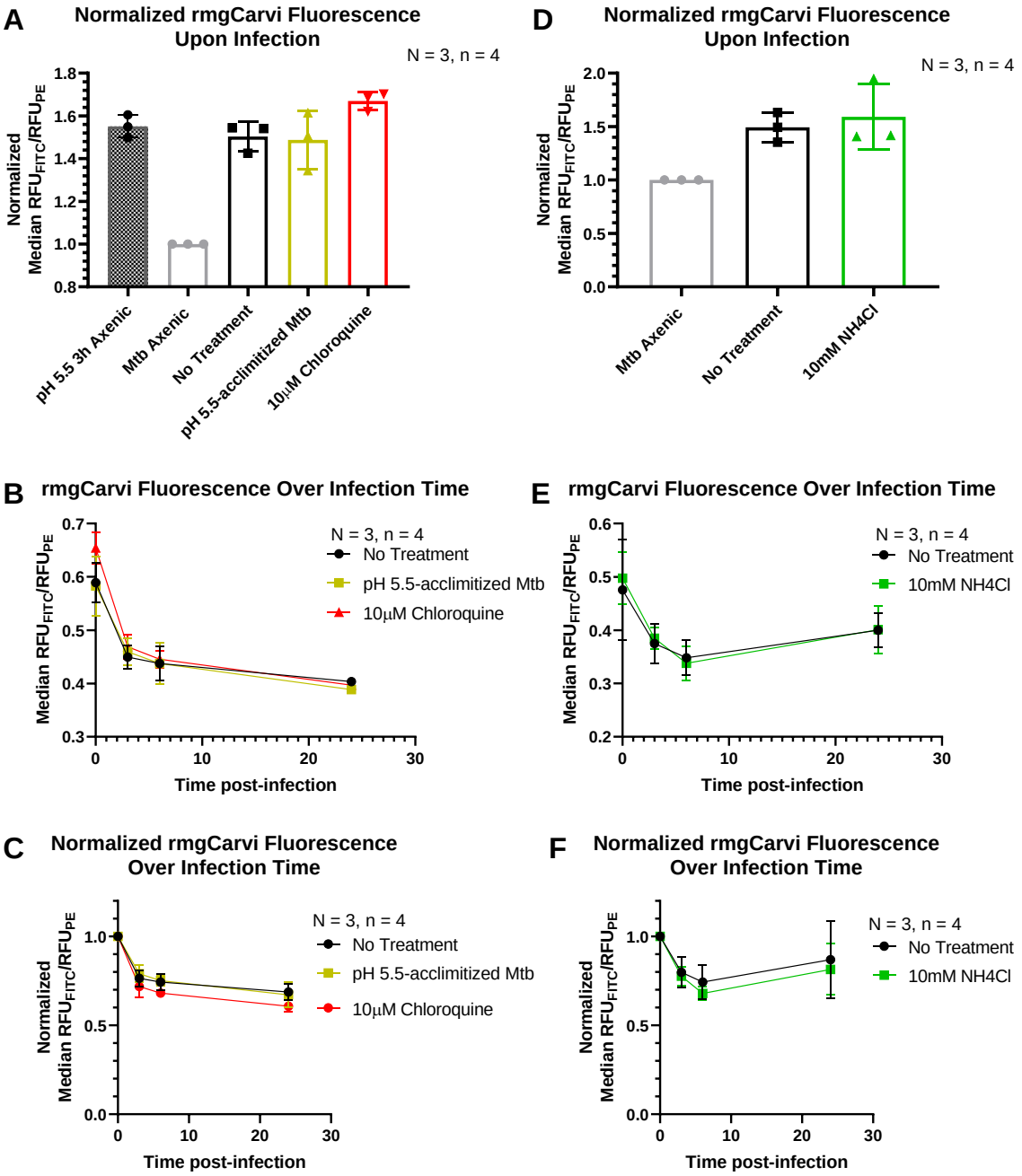

Figure 12: *The acidic environment of the early phagosome is not the primary driver of elevated intramycobacterial cAMP upon infection.* Intramycobacterial cAMP levels were assayed using rmgCarvi fluorescence after the incubation period of macrophage infection (**A**, **D**) and over infection time (**B** and **E,** represent the ratio of median FITC to median PE fluorescence; **C**, represent the same value normalized to that at the 0-hour post-infection timepoint). The error bars represent the standard deviation.

4.4. *Insights into Host-Pathogen Interactions: Arriving at Basic Principles of cAMP Signalling in Mycobacterium tuberculosis During Infection in RAW 264.7 Macrophages*

The infection experiments conducted with rmgCarvi expressing Mtb revealed the following novel insights into certain basic principles of cAMP signalling during Mtb infection in RAW 264.7 macrophages.

1. There exists a single burst of cAMP into the host macrophage with tight temporal control.

In all the results discussed up to this point, there exists a robust reduction in intramycobacterial cAMP levels at 3 hours post-infection, irrespective of treatment condition, corresponding exactly with the timepoint at which previous studies in the field have reported a burst of cAMP into the macrophage from Mtb (Agarwal *et al.*, 2009; Bai *et al.*, 2009). However, the state of intramycobacterial cAMP between the 6- and 24-hour timepoints remained an unknown entity. A single experiment (wherein two treatment conditions of ammonium chloride and IFN-γ-activated macrophages were present) was carried out to assay intramycobacterial cAMP levels at 3-hour intervals post-infection (**Figures 13A** and **13B**).

A tight temporal control in the expulsion of cAMP out of the Mtb was observed. The cAMP expulsion was seen to take place within a very short time period between the 2h40min and 3h30min timepoints post-infection. This indicates that Mtb builds up a pool of dispensable cytosolic cAMP, following which it expels the majority of it out into the host macrophage in a short time window lasting about 45 minutes. The cAMP burst is seen to continue till the 6-hour post-infection timepoint following which intramycobacterial cAMP levels recover and increase to a maximal value and reduce only after 18 hours post-infection. This indicates the presence of a temporal control on the conclusion of the cAMP burst into the macrophage as well, likely linked to the de-acidification of the phagosome by Mtb.

2. Conserved upper and lower bounds to intramycobacterial cAMP during infection.

As can be observed from **Figures 9B, 10B, 11B, 12B, 12E**, and **13A**, which report the ratio of median FITC fluorescence to median PE fluorescence of the biosensor during infection time (and not the value of the same normalized to that at 0-hours of infection),

there exists a rather conserved lower bound on the intramycobacterial cAMP level once the cAMP burst into the macrophage has occured. This value of the ratio between 0.35 and 0.4 is consistent across experiments and treatment conditions. Similarly, as can be seen from **Figure 13A**, there is also a conserved upper bound to intramycobacterial cAMP levels during infection.

These observations indicate an important aspect of the nature of control over cAMP levels in Mtb during infection in a host. It is very likely that deviations from these upper and lower bounds of intramycobacterial cAMP are detrimental to Mtb survival, at least during the first 24 hours of infection in RAW 264.7 macrophages. These results provide the impetus for further experiments making use of time-lapse microscopy in combination with the rmgCarvi cAMP biosensor to investigate the nature of these processes visually, in real-time.

3. cAMP export from Mtb in response to physiologically relevant stresses *in vitro*

The observed reduction in intramycobacterial cAMP levels at 6 hours post-exposure to the acid and salt stress observed in **Figure 8** seems puzzling when analysed in isolation. However, when considered through an evolutionary lens, the presence of the phenomenon is logical. 6 hours of exposure to a stress corresponds temporally to the 3 hours post-infection timepoint (since it represents around 6 hours after Mtb, and the macrophages were introduced to each other, and Mtb was likely internalised). Upon being exposed to a physiologically relevant stress *in vitro*, Mtb's cAMP response is one that has been shaped evolutionarily – by its interaction with the host cell that is its primary niche, the macrophage. Therefore, the cAMP response to any physiologically relevant stress, if assessed *in vitro*, will likely follow a similar temporal pattern wherein there is an initial increase in intramycobacterial cAMP (the kinetics of which will be governed by the modality of the cAMP induction – protein activity modulation by phospho-signalling or two-component systems, or steady state protein level modulation by a transcriptional response) followed by cAMP export out into the surrounding environment (media if *in vitro,* host cell if during an infection).

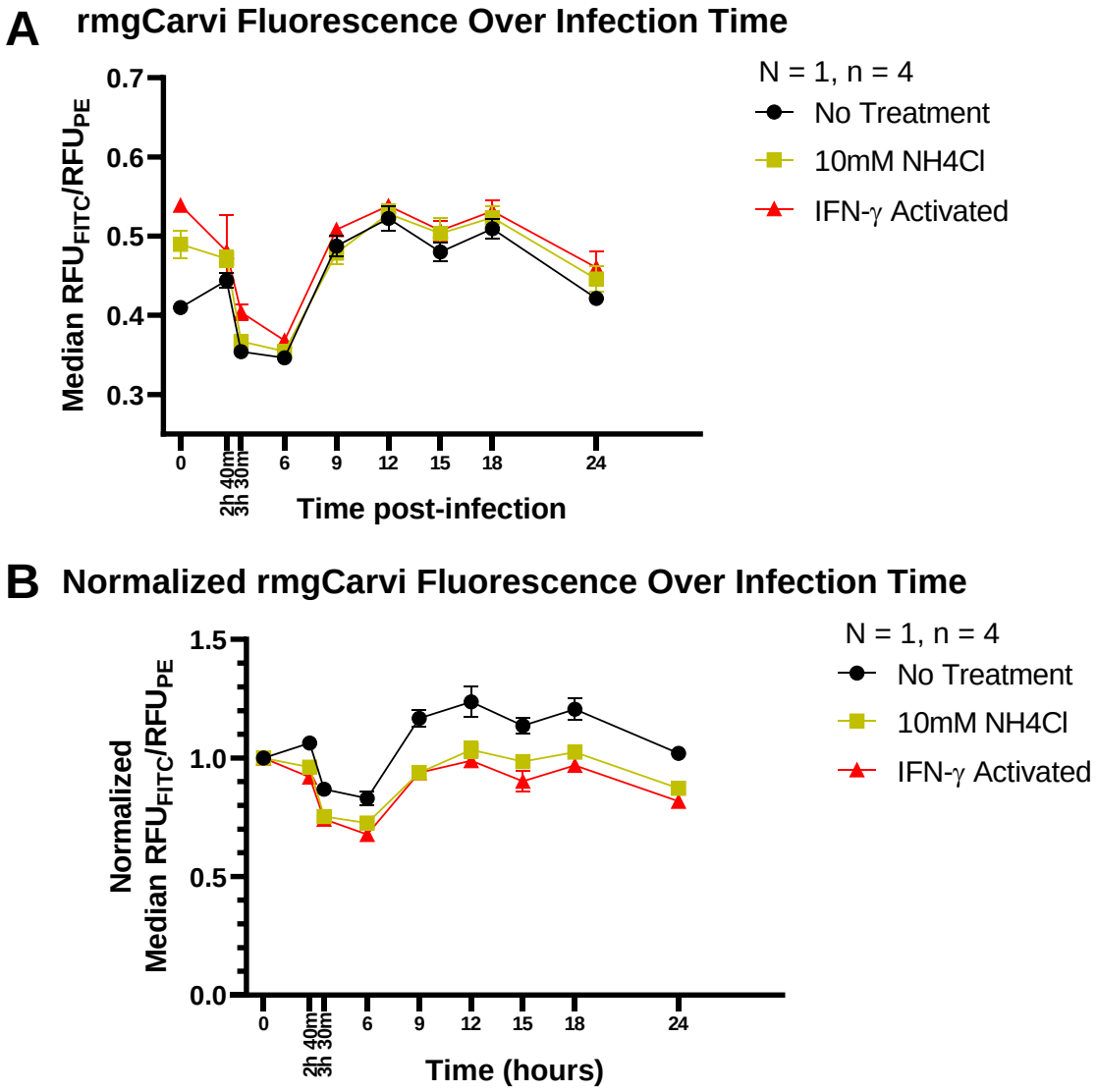

Figure 13: *Investigating Intramycobacterial cAMP Levels Every 3 hours Post-Infection in RAW 264.7 Macrophages.* Intramycobacterial cAMP levels were assayed using rmgCarvi fluorescence over infection time. **A** represents the ratio of median FITC to median PE fluorescence and **B** represents the same value normalized to that at the 0-hour post-infection timepoint. The error bars represent the standard deviation.

Chapter 4 **Conclusion**

Over the course of the thesis, the multiple experiments conducted using rmgCarvi to monitor intramycobacterial cAMP levels have helped display the powerful utility of the biosensor to study cAMP signalling in *Mycobacterium tuberculosis.*

In the first section, by leveraging rmgCarvi, we report the nature of intramycobacterial cAMP during regular axenic growth of *M. tuberculosis* for the first time. In the second section, we successfully identified the presence of a surge in intramycobacterial cAMP levels upon resuscitation from dormancy. These findings not only validate results reported in previous studies (Shleeva *et al.*, 2013, 2017) but also expand on them by identifying the phenomenon's exogenous free fatty acid-independent nature. Additionally, the kinetics of this phenomenon that we uncovered likely point to the presence of an unidentified nutrient signalling pathway that results in *de novo* cAMP synthesis in response to glycerol and/or glucose as carbon sources. In the third section, we report on the temporality of the cAMP response to acid and salt stresses. These results validate previous reports of the same (Rebollo-Ramirez and Larrouy-Maumus, 2019; Khan *et al.*, 2024) and indicate the presence of a synergistic regulation of cAMP levels in response to these physiologically relevant stresses, as has been reported in the case of virulence determining genes (Tan *et al.*, 2013; Khan *et al.*, 2022). The results also provide the impetus to investigate the mechanism by which the transcriptional regulator CRP modulates cAMP levels. In the fourth section, we uncovered the temporal dynamics of intramycobacterial cAMP during infection in RAW 264.7 macrophages, a novel addition to the field. The results are in strong agreement with previous studies that report an increase in intramycobacterial cAMP upon infection in macrophages and a subsequent cAMP burst into the macrophage (Agarwal *et al.*, 2009; Bai *et al.*, 2009). Our results identify the presence of tight temporal control over the inception and conclusion of the cAMP burst and conserved upper and lower bounds of intramycobacterial cAMP during infection. These results provide the foundation to assay cAMP levels during infection in real-time using rmgCarvi in combination with time-lapse microscopy. Additionally, it indicates the existence of currently unknown players in the cAMP signalling network of Mtb that serve to sense intramycobacterial cAMP levels and maintain them at optimal values. Most strikingly, our results indicate that the acidic pH of the phagosome is not a

requirement for the increased intramycobacterial cAMP production upon infection and subsequent burst into the host macrophage. The nature of the intramycobacterial cAMP response to infection in non-professional phagocytic cells, such as epithelial cells, might provide interesting insights into this phenomenon.

Put together, our results uncover fundamental insights into certain basic principles of cAMP signalling in *Mycobacterium tuberculosis* and directs the course for future experiments to better understand the cAMP signalling network and its regulation. An improved understanding of this can lead to the development of improved therapeutic avenues, as has already been explored with the adenylate cyclase agonist V-59, which has been shown to improve survival outcomes of infected mice (Wilburn *et al.*, 2022).

References

Portions of the introduction have been adapted from a review article authored by Srivathsa S Kurpad and Neeraj Dhar. The manuscript for the same has been submitted to ACS Infectious Diseases and is currently under revision.

Abdel Motaal, A, Tews, I, Schultz, JE, and Linder, JU (2006). Fatty acid regulation of adenylyl cyclase Rv2212 from Mycobacterium tuberculosis H37Rv. FEBS J 273, 4219–4228.

Abramovitch, RB, Rohde, KH, Hsu, F-F, and Russell, DG (2011). aprABC: a Mycobacterium tuberculosis complex-specific locus that modulates pH-driven adaptation to the macrophage phagosome. Molecular Microbiology 80, 678–694.

Agarwal, N, Lamichhane, G, Gupta, R, Nolan, S, and Bishai, WR (2009). Cyclic AMP intoxication of macrophages by a Mycobacterium tuberculosis adenylate cyclase. Nature 460, 98–102.

Al-Bari, MdAA (2017). Targeting endosomal acidification by chloroquine analogs as a promising strategy for the treatment of emerging viral diseases. Pharmacology Research & Perspectives 5, e00293.

Altarejos, JY, and Montminy, M (2011). CREB and the CRTC co-activators: sensors for hormonal and metabolic signals. Nat Rev Mol Cell Biol 12, 141–151.

Alvarez, AF, and Georgellis, D (2023). Environmental adaptation and diversification of bacterial two-component systems. Current Opinion in Microbiology 76, 102399.

Anderson, CJ, Satkovich, J, Köseoğlu, VK, Agaisse, H, and Kendall, MM (2018). The Ethanolamine Permease EutH Promotes Vacuole Adaptation of Salmonella enterica and Listeria monocytogenes during Macrophage Infection. Infection and Immunity 86, 10.1128/iai.00172-18.

Armitage, JP (1992). Behavioral responses in bacteria. Annu Rev Physiol 54, 683–714.

Bai, G, McCue, LA, and McDonough, KA (2005). Characterization of Mycobacterium tuberculosis Rv3676 (CRPMt), a Cyclic AMP Receptor Protein-Like DNA Binding Protein. Journal of Bacteriology 187, 7795–7804.

Bai, G, Schaak, DD, and McDonough, KA (2009). cAMP levels within Mycobacterium tuberculosis and M. bovis BCG increase upon infection of macrophages. FEMS Immunol Med Microbiol 55, 68–73.

Banerjee, A, Adolph, RS, Gopalakrishnapai, J, Kleinboelting, S, Emmerich, C, Steegborn, C, and Visweswariah, SS (2015). A Universal Stress Protein (USP) in Mycobacteria Binds cAMP. Journal of Biological Chemistry 290, 12731–12743.

Banerjee, A, Chakraborty, M, Sharma, S, Chaturvedi, R, Bose, A, Biswas, P, Singh, A, and Visweswariah, SS (2024). Cyclic AMP binding to a universal stress protein in Mycobacterium tuberculosis is essential for viability. Journal of Biological Chemistry 300.

Bansal, R, Anil Kumar, V, Sevalkar, RR, Singh, PR, and Sarkar, D (2017). Mycobacterium tuberculosis virulence-regulator PhoP interacts with alternative sigma factor SigE during acid-stress response. Molecular Microbiology 104, 400–411.

Betts, JC, Lukey, PT, Robb, LC, McAdam, RA, and Duncan, K (2002). Evaluation of a nutrient starvation model of Mycobacterium tuberculosis persistence by gene and protein expression profiling. Mol Microbiol 43, 717–731.

Block, AM, Namugenyi, SB, Palani, NP, Brokaw, AM, Zhang, L, Beckman, KB, and Tischler, AD (2023). Mycobacterium tuberculosis Requires the Outer Membrane Lipid Phthiocerol Dimycocerosate for Starvation-Induced Antibiotic Tolerance. mSystems 8, e00699-22.

Chao, J, Wong, D, Zheng, X, Poirier, V, Bach, H, Hmama, Z, and Av-Gay, Y (2010). Protein kinase and phosphatase signaling in *Mycobacterium tuberculosis* physiology and pathogenesis. Biochimica et Biophysica Acta (BBA) - Proteins and Proteomics 1804, 620–627.

Coban, C (2020). The host targeting effect of chloroquine in malaria. Current Opinion in Immunology 66, 98–107.

Conte, MP, Petrone, G, Longhi, C, Valenti, P, Morelli, R, Superti, F, and Seganti, L (1996). The effects of inhibitors of vacuolar acidification on the release of Listeria monocytogenes from phagosomes of Caco-2 cells. Journal of Medical Microbiology 44, 418–424.

Cortes, T, Schubert, OT, Rose, G, Arnvig, KB, Comas, I, Aebersold, R, and Young, DB (2013). Genome-wide Mapping of Transcriptional Start Sites Defines an Extensive Leaderless Transcriptome in *Mycobacterium tuberculosis*. Cell Reports 5, 1121–1131.

D'Ari, R, Jaffé, A, Bouloc, P, and Robin, A (1988). Cyclic AMP and cell division in Escherichia coli. Journal of Bacteriology 170, 65–70.

Dass, BKM, Sharma, R, Shenoy, AR, Mattoo, R, and Visweswariah, SS (2008). Cyclic AMP in Mycobacteria: Characterization and Functional Role of the Rv1647 Ortholog in Mycobacterium smegmatis. J Bacteriol 190, 3824–3834.

Dey, B, and Bishai, WR (2014). Crosstalk between Mycobacterium tuberculosis and the host cell. Seminars in Immunology 26, 486–496.

Eum, S-Y, Kong, J-H, Hong, M-S, Lee, Y-J, Kim, J-H, Hwang, S-H, Cho, S-N, Via, LE, and Barry, CE (2010). Neutrophils Are the Predominant Infected Phagocytic Cells in the Airways of Patients With Active Pulmonary TB. Chest 137, 122–128.

Gazdik, MA, Bai, G, Wu, Y, and McDonough, KA (2009). Rv1675c (cmr) regulates intramacrophage and cyclic AMP-induced gene expression in Mycobacterium tuberculosis-complex mycobacteria. Mol Microbiol 71, 434–448.

Gold, B, and Nathan, C (2017). Targeting Phenotypically Tolerant Mycobacterium tuberculosis. Microbiology Spectrum 5, 10.1128/microbiolspec.tbtb2-0031–2016.

Golding, I, Paulsson, J, Zawilski, SM, and Cox, EC (2005). Real-Time Kinetics of Gene Activity in Individual Bacteria. Cell 123, 1025–1036.

Gordon, VD, and Wang, L (2019). Bacterial mechanosensing: the force will be with you, always. Journal of Cell Science 132, jcs227694.

Görke, B, and Stülke, J (2008). Carbon catabolite repression in bacteria: many ways to make the most out of nutrients. Nat Rev Microbiol 6, 613–624.

Harada, K, Ito, M, Wang, X, Tanaka, M, Wongso, D, Konno, A, Hirai, H, Hirase, H, Tsuboi, T, and Kitaguchi, T (2017). Red fluorescent protein-based cAMP indicator applicable to optogenetics and in vivo imaging. Sci Rep 7, 7351.

Hart, PD, and Young, MR (1991). Ammonium chloride, an inhibitor of phagosome-lysosome fusion in macrophages, concurrently induces phagosome-endosome fusion, and opens a novel pathway: studies of a pathogenic mycobacterium and a nonpathogenic yeast. Journal of Experimental Medicine 174, 881–889.

Hart, PD, Young, MR, Jordan, MM, Perkins, WJ, and Geisow, MJ (1983). Chemical inhibitors of phagosome-lysosome fusion in cultured macrophages also inhibit saltatory lysosomal movements. A combined microscopic and computer study. Journal of Experimental Medicine 158, 477–492.

Hatzios, SK, Baer, CE, Rustad, TR, Siegrist, MS, Pang, JM, Ortega, C, Alber, T, Grundner, C, Sherman, DR, and Bertozzi, CR (2013). Osmosensory signaling in Mycobacterium tuberculosis mediated by a eukaryotic-like Ser/Thr protein kinase. Proceedings of the National Academy of Sciences 110, E5069–E5077.

Hengge, R (2009). Principles of c-di-GMP signalling in bacteria. Nat Rev Microbiol 7, 263–273.

Huang, L, Nazarova, EV, and Russell, DG (2019). Mycobacterium tuberculosis: Bacterial Fitness within the Host Macrophage. Microbiology Spectrum 7, 10.1128/microbiolspec.bai-0001–2019.

Huynh, KK, and Grinstein, S (2007). Regulation of Vacuolar pH and Its Modulation by Some Microbial Species. Microbiology and Molecular Biology Reviews 71, 452–462.

Jaishankar, J, and Srivastava, P (2017). Molecular Basis of Stationary Phase Survival and Applications. Front Microbiol 8.

Johnson, RM, and McDonough, KA (2018). Cyclic nucleotide signaling in Mycobacterium tuberculosis: an expanding repertoire. Pathog Dis 76, fty048.

Jouanguy, E, Lamhamedi-Cherradi, S, Lammas, D, Dorman, SE, Fondanèche, M-C, Dupuis, S, Döffinger, R, Altare, F, Girdlestone, J, Emile, J-F, *et al.* (1999). A human IFNGR1 small deletion hotspot associated with dominant susceptibility to mycobacterial infection. Nat Genet 21, 370–378.

Kahramanoglou, C, Cortes, T, Matange, N, Hunt, DM, Visweswariah, SS, Young, DB, and Buxton, RS (2014). Genomic mapping of cAMP receptor protein (CRPMt) in Mycobacterium tuberculosis: relation to transcriptional start sites and the role of CRPMt as a transcription factor. Nucleic Acids Research 42, 8320–8329.

Kak, G, Raza, M, and Tiwari, BK (2018). Interferon-gamma (IFN-γ): Exploring its implications in infectious diseases. Biomolecular Concepts 9, 64–79.

Kalamidas, SA, Kuehnel, MP, Peyron, P, Rybin, V, Rauch, S, Kotoulas, OB, Houslay, M, Hemmings, BA, Gutierrez, MG, Anes, E, *et al.* (2006). cAMP synthesis and degradation by phagosomes regulate actin assembly and fusion events: consequences for mycobacteria. J Cell Sci 119, 3686–3694.

Kawata, S, Mukai, Y, Nishimura, Y, Takahashi, T, and Saitoh, N (2022). Green fluorescent cAMP indicator of high speed and specificity suitable for neuronal live-cell imaging. Proceedings of the National Academy of Sciences 119, e2122618119.

Keppetipola, N, and Shuman, S (2008). A Phosphate-binding Histidine of Binuclear Metallophosphodiesterase Enzymes Is a Determinant of 2′,3′-Cyclic Nucleotide Phosphodiesterase Activity*. Journal of Biological Chemistry 283, 30942–30949.

Khan, H, Paul, P, Goar, H, Bamniya, B, Baid, N, and Sarkar, D (2024). Mycobacterium tuberculosis PhoP integrates stress response to intracellular survival by regulating cAMP level. eLife 13, RP92136.

Khan, H, Paul, P, Sevalkar, RR, Kachhap, S, Singh, B, and Sarkar, D (2022). Convergence of two global regulators to coordinate expression of essential virulence determinants of Mycobacterium tuberculosis. eLife 11, e80965.

Kim, JW, Roberts, CD, Berg, SA, Caicedo, A, Roper, SD, and Chaudhari, N (2008). Imaging Cyclic AMP Changes in Pancreatic Islets of Transgenic Reporter Mice. PLOS ONE 3, e2127.

Knapp, GS, and McDonough, KA (2014). Cyclic AMP Signaling in Mycobacteria. Microbiol Spectr 2.

Kresge, N, Simoni, RD, and Hill, RL (2005). Earl W. Sutherland's Discovery of Cyclic Adenine Monophosphate and the Second Messenger System. Journal of Biological Chemistry 280, e39–e40.

Larrouy-Maumus, G, Marino, LB, Madduri, AVR, Ragan, TJ, Hunt, DM, Bassano, L, Gutierrez, MG, Moody, DB, Pavan, FR, and de Carvalho, LPS (2016). Cell-Envelope Remodeling as a Determinant of Phenotypic Antibacterial Tolerance in Mycobacterium tuberculosis. ACS Infect Dis 2, 352–360.

Laub, MT, and Goulian, M (2007). Specificity in Two-Component Signal Transduction Pathways. Annual Review of Genetics 41, 121–145.

Lee, W, VanderVen, BC, Fahey, RJ, and Russell, DG (2013). Intracellular Mycobacterium tuberculosis exploits host-derived fatty acids to limit metabolic stress. J Biol Chem 288, 6788–6800.

Leopold Wager, CM, Bonifacio, JR, Simper, J, Naoun, AA, Arnett, E, and Schlesinger, LS (2023). Activation of transcription factor CREB in human macrophages by Mycobacterium tuberculosis promotes bacterial survival, reduces NF-kB nuclear transit and limits phagolysosome fusion by reduced necroptotic signaling. PLoS Pathog 19, e1011297.

Lerner, TR, Borel, S, Greenwood, DJ, Repnik, U, Russell, MRG, Herbst, S, Jones, ML, Collinson, LM, Griffiths, G, and Gutierrez, MG (2017). Mycobacterium tuberculosis replicates within necrotic human macrophages. J Cell Biol 216, 583–594.

Mauthe, M, Orhon, I, Rocchi, C, Zhou, X, Luhr, M, Hijlkema, K-J, Coppes, RP, Engedal, N, Mari, M, and Reggiori, F (2018). Chloroquine inhibits autophagic flux by decreasing autophagosome-lysosome fusion. Autophagy 14, 1435–1455.

McDonough, KA, and Rodriguez, A (2011). The myriad roles of cyclic AMP in microbial pathogens: from signal to sword. Nat Rev Microbiol 10, 27–38.

McDowell, JR, Bai, G, Lasek-Nesselquist, E, Eisele, LE, Wu, Y, Hurteau, G, Johnson, R, Bai, Y, Chen, Y, Chan, J, *et al.* (2023). Mycobacterial phosphodiesterase Rv0805 is a virulence determinant and its cyclic nucleotide hydrolytic activity is required for propionate detoxification. Molecular Microbiology 119, 401–422.

Mishra, R, Kohli, S, Malhotra, N, Bandyopadhyay, P, Mehta, M, Munshi, M, Adiga, V, Ahuja, VK, Shandil, RK, Rajmani, RS, *et al.* (2019). Targeting redox heterogeneity to counteract drug tolerance in replicating Mycobacterium tuberculosis. Science Translational Medicine 11, eaaw6635.

Mitosch, K, Rieckh, G, and Bollenbach, T (2019). Temporal order and precision of complex stress responses in individual bacteria. Molecular Systems Biology 15, e8470.

Nambi, S, Gupta, K, Bhattacharyya, M, Ramakrishnan, P, Ravikumar, V, Siddiqui, N, Thomas, AT, and Visweswariah, SS (2013). Cyclic AMP-dependent protein lysine acylation in mycobacteria regulates fatty acid and propionate metabolism. J Biol Chem 288, 14114–14124.

Nazarova, EV, Montague, CR, Huang, L, La, T, Russell, D, and VanderVen, BC (2019). The genetic requirements of fatty acid import by Mycobacterium tuberculosis within macrophages. eLife 8, e43621.

Newton, AC, Bootman, MD, and Scott, JD (2016). Second Messengers. Cold Spring Harb Perspect Biol 8, a005926.

Pandey, AK, and Sassetti, CM (2008). Mycobacterial persistence requires the utilization of host cholesterol. Proc Natl Acad Sci U S A 105, 4376–4380.

Parish, T (2014). Two-Component Regulatory Systems of Mycobacteria. Microbiology Spectrum 2, 10.1128/microbiolspec.mgm2-0010–2013.

Persat, A, Inclan, YF, Engel, JN, Stone, HA, and Gitai, Z (2015). Type IV pili mechanochemically regulate virulence factors in Pseudomonas aeruginosa. Proceedings of the National Academy of Sciences 112, 7563–7568.

Philips, JA, and Ernst, JD (2012). Tuberculosis pathogenesis and immunity. Annu Rev Pathol 7, 353–384.

Porter, SL, Wadhams, GH, and Armitage, JP (2011). Signal processing in complex chemotaxis pathways. Nat Rev Microbiol 9, 153–165.

Prisic, S, and Husson, RN (2014). Mycobacterium tuberculosis Serine/Threonine Protein Kinases. Microbiology Spectrum 2, 10.1128/microbiolspec.mgm2-0006–2013.

Rebollo-Ramirez, S, and Larrouy-Maumus, G (2019). NaCl triggers the CRP-dependent increase of cAMP in *Mycobacterium tuberculosis*. Tuberculosis 116, 8–16.

Reniere, ML, Whiteley, AT, and Portnoy, DA (2016). An In Vivo Selection Identifies Listeria monocytogenes Genes Required to Sense the Intracellular Environment and Activate Virulence Factor Expression. PLOS Pathogens 12, e1005741.

Rickman, L, Scott, C, Hunt, DM, Hutchinson, T, Menéndez, MC, Whalan, R, Hinds, J, Colston, MJ, Green, J, and Buxton, RS (2005). A member of the cAMP receptor protein family of transcription regulators in Mycobacterium tuberculosis is required for virulence in mice and controls transcription of the rpfA gene coding for a resuscitation promoting factor. Mol Microbiol 56, 1274–1286.

Rohde, K, Yates, RM, Purdy, GE, and Russell, DG (2007). Mycobacterium tuberculosis and the environment within the phagosome. Immunological Reviews 219, 37–54.

Russell, DG, Cardona, P-J, Kim, M-J, Allain, S, and Altare, F (2009). Foamy macrophages and the progression of the human tuberculosis granuloma. Nat Immunol 10, 943–948.

Russell, DG, Huang, L, and VanderVen, BC (2019). Immunometabolism at the interface between macrophages and pathogens. Nat Rev Immunol 19, 291–304.

Sawyer, EB, Phelan, JE, Clark, TG, and Cortes, T (2021). A snapshot of translation in Mycobacterium tuberculosis during exponential growth and nutrient starvation revealed by ribosome profiling. Cell Reports 34.

Schroder, K, Hertzog, PJ, Ravasi, T, and Hume, DA (2004). Interferon-γ: an overview of signals, mechanisms and functions. Journal of Leukocyte Biology 75, 163–189.

Serezani, CH, Ballinger, MN, Aronoff, DM, and Peters-Golden, M (2008). Cyclic AMP. Am J Respir Cell Mol Biol 39, 127–132.

Shenoy, AR, Capuder, M, Draškovič, P, Lamba, D, Visweswariah, SS, and Podobnik, M (2007). Structural and Biochemical Analysis of the Rv0805 Cyclic Nucleotide Phosphodiesterase from *Mycobacterium tuberculosis*. Journal of Molecular Biology 365, 211–225.

Shleeva, M, Goncharenko, A, Kudykina, Y, Young, D, Young, M, and Kaprelyants, A (2013). Cyclic Amp-Dependent Resuscitation of Dormant Mycobacteria by Exogenous Free Fatty Acids. PLOS ONE 8, e82914.

Shleeva, MO, Kondratieva, TK, Demina, GR, Rubakova, EI, Goncharenko, AV, Apt, AS, and Kaprelyants, AS (2017). Overexpression of Adenylyl Cyclase Encoded by the Mycobacterium tuberculosis Rv2212 Gene Confers Improved Fitness, Accelerated Recovery from Dormancy and Enhanced Virulence in Mice. Frontiers in Cellular and Infection Microbiology 7.

Stupar, M, Furness, J, De Voss, CJ, Tan, L, and West, NP (2022). Two-component sensor histidine kinases of Mycobacterium tuberculosis: Beacons for niche navigation. Molecular Microbiology 117, 973–985.

Tan, S, Sukumar, N, Abramovitch, RB, Parish, T, and Russell, DG (2013). Mycobacterium tuberculosis Responds to Chloride and pH as Synergistic Cues to the Immune Status of its Host Cell. PLOS Pathogens 9, e1003282.

Thakur, A, Mikkelsen, H, and Jungersen, G (2019). Intracellular Pathogens: Host Immunity and Microbial Persistence Strategies. J Immunol Res 2019, 1356540.

Thomson, M, Liu, Y, Nunta, K, Cheyne, A, Fernandes, N, Williams, R, Garza-Garcia, A, and Larrouy-Maumus, G (2022). Expression of a novel mycobacterial phosphodiesterase successfully lowers cAMP levels resulting in reduced tolerance to cell wall–targeting antimicrobials. J Biol Chem 298, 102151.

Thorner, J, Hunter, T, Cantley, LC, and Sever, R (2014). Signal Transduction: From the Atomic Age to the Post-Genomic Era. Cold Spring Harb Perspect Biol 6, a022913.

Toniolo, C, Rutschmann, O, and McKinney, JD (2021). Do chance encounters between heterogeneous cells shape the outcome of tuberculosis infections? Current Opinion in Microbiology 59, 72–78.

Wilburn, KM, Montague, CR, Qin, B, Woods, AK, Love, MS, McNamara, CW, Schultz, PG, Southard, TL, Huang, L, Petrassi, HM, *et al.* (2022). Pharmacological and genetic activation of cAMP synthesis disrupts cholesterol utilization in Mycobacterium tuberculosis. PLoS Pathog 18, e1009862.

Wong, AI, Beites, T, Planck, KA, Fieweger, RA, Eckartt, KA, Li, S, Poulton, NC, VanderVen, BC, Rhee, KY, Schnappinger, D, *et al.* (2023). Cyclic AMP is a critical mediator of intrinsic drug resistance and fatty acid metabolism in M. tuberculosis. eLife 12, e81177.

Xie, Z, Siddiqi, N, and Rubin, EJ (2005). Differential Antibiotic Susceptibilities of Starved Mycobacterium tuberculosis Isolates. Antimicrobial Agents and Chemotherapy 49, 4778–4780.

Yamamoto, K, Hirao, K, Oshima, T, Aiba, H, Utsumi, R, and Ishihama, A (2005). Functional Characterization *in Vitro* of All Two-component Signal Transduction Systems from *Escherichia coli**. Journal of Biological Chemistry 280, 1448–1456.

Yates, RM, Hermetter, A, and Russell, DG (2005). The Kinetics of Phagosome Maturation as a Function of Phagosome/Lysosome Fusion and Acquisition of Hydrolytic Activity. Traffic 6, 413–420.

Zaccolo, M (2022). cAMP Signaling: Methods and Protocols, New York, NY: Springer US.

Zaccolo, M, De Giorgi, F, Cho, CY, Feng, L, Knapp, T, Negulescu, PA, Taylor, SS, Tsien, RY, and Pozzan, T (2000). A genetically encoded, fluorescent indicator for cyclic AMP in living cells. Nat Cell Biol 2, 25–29.

Supplementary Information

A **mCherry Fluorescence During Rescue from Deep Stationary Phase in 7H9 + ADC**

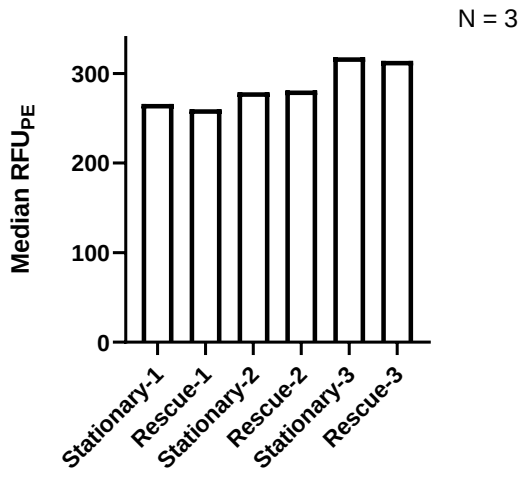

B **mCherry Fluorescence During Rescue from Deep Stationary Phase in 7H9 + OADC**

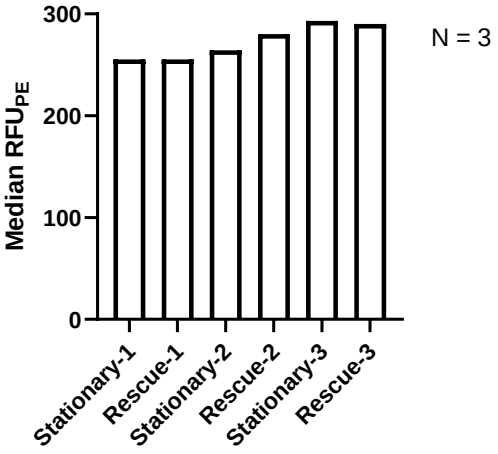

C **mCherry Fluorescence During Resuscitation from Nutrient Starvation-Induced Dormancy**

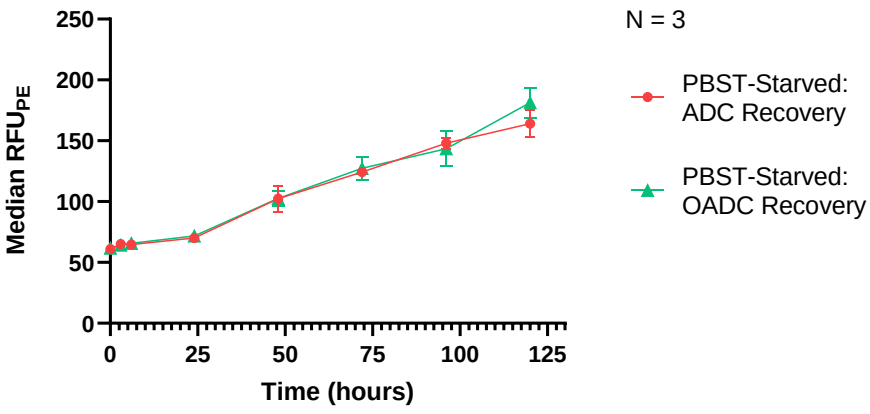

Supplementary Figure 1: *mCherry fluorescence levels does not dramatically increase shortly after rescue from dormancy and dormancy-like states.* mCherry fluorescence was assayed after 3 hours of Msm's rescue from deep-stationary phase in 7H9 supplemented with ADC (**A**) or OADC (**B**) and over the course of Mtb's rescue from nutrient starvation-induced dormancy (**C**). The error bars represent the standard deviation.